

Dear Editor, Dr. Michael Weintraub,

Dear reviewers,

We are happy to provide the revised version of the manuscript *bg-2019-292*. As a result of the reviewers' comments, we made some major changes. These include the way we address DRIFTS "peak areas" which are now correctly called areas below absorbance bands. We also corrected the wording for the 1620 cm<sup>-1</sup> band to aromatic/carboxylate which, due to higher specificity, we prefer to the suggestion of unsaturated carbon. In response to the comments of reviewer 4, we also clarified the concept of the DSI and how it is translated into an equation for SOM model pool partitioning. More details on the soil sampling and analysis were added, as was requested. We addressed all reviewers' comments and made the required changes based on these comments to the manuscript. We hope that with these recent changes, the manuscript now has the quality to be accepted for Biogeosciences.

We combined the responses to all authors in this PDF. Responses are in **blue color**, and a preview of changes made to the text in **green color**. The uploaded manuscript consists of a clean version, the version with tracked changes is attached at the end of this document.

We thank you for your effort in handling the manuscript during the review process.

On behalf of all coauthors,

Moritz Laub

**Lauric Cécillon:**

Dear authors, dear colleagues,

I thank you for your efforts to improve your revised draft and for testing new calculations (linking DSI and CPsoc). Incorporating such information as supplementary information is suitable to the readers of Biogeosciences.

I have one "technical", yet important comment on your revised draft.

In my view, naming as "aromatic C=C" the 1660-1580 cm<sup>-1</sup> DRIFT region that is integrated around the 1620 cm<sup>-1</sup> peak is not acceptable.

In my previous comments on your draft, I mostly emphasized on mineral artifacts in this DRIFT spectral region, so that the DSI is not carrying an information that is only linked to organic carbon.

But we know that C=O bounds are also absorbing energy on the 1660 cm<sup>-1</sup> side of this DRIFT spectral region (as acknowledged by Demyan et al., 2012 in EJSS, <https://doi.org/10.1111/j.1365-2389.2011.01420.x>).

So beside mineral (+ water) artifacts, the 1660-1580 cm<sup>-1</sup> DRIFT region represent a mixture of C=C + C=O carbon.

It thus not acceptable to name this region "aromatic carbon". This would make readers erroneously think that aromatic carbon is making the major part of stable carbon in soils, which is not true as stable carbon is generally richer in O than bulk SOM (except in soils rich in charcoals).

Thus I ask you to change the naming of the DRIFT 1660-1580 cm<sup>-1</sup> spectral region to a proper (and scientifically correct) one such as "unsaturated carbon" (with C=O and C=C bounds ; see e.g. the Figure 1 of Pengerud et al., 2013 in Ecosystems, <https://doi.org/10.1007/s10021-013-9652-5>).

I am looking forward to reading the final and accepted version of your draft in Biogeosciences.

Kind regards,

Lauric Cécillon

Dear Lauric Cécillon,

Thank you for this very constructive and helpful suggestion. We agree that considering the involvement of C=O bonds in our defined 1620 cm<sup>-1</sup> absorbance band is appropriate, and hence changed the name of the absorbance band to aromatic/carboxylate throughout the manuscript. While we recognize that chemically the different functional groups we use are either unsaturated (C=C/C=O) or saturated (C-H), we feel that, specifying the vibrational assignments (e.g. aliphatic and aromatic/carboxylate) may avoid confusion with additional unsaturated functional groups in addition to C=C/C=O groups and provide clarity. Additionally, our band area of 1660-1580 cm<sup>-1</sup> does not correspond to the much larger band area of 1800 –1525 cm<sup>-1</sup>, used by (Pengerud et al., 2013). As previously mentioned, we have clarified that the 1620 cm<sup>-1</sup> band includes both C=C and C=O functional groups.

Regards

## Reviewer 2:

I criticized in my earlier review that Laub and colleagues use the chemical recalcitrance hypothesis to explain SOM cycling. Now, they cite an earlier study that their index, which is based on the aromatic and aliphatic peaks, is correlated with aggregation.

Mechanistically, the interpretation should be chemical recalcitrance. I don't get what we learn from DRIFTS spectra when we deviate from the mechanistic interpretation. Demyan et al. (2012) suggest a relation to mineral-association (correlation to the sum of the heavy fraction  $> 1.8 \text{ g cm}^{-3}$  and clay fraction compared to light fraction  $< 1.8 \text{ g cm}^{-3}$ ) and not to aggregation (the occluded light fraction is not measured in that study).

Arguably microaggregate occluded soil organic matter can be a part of the abovementioned heavy fraction  $> 1.8 \text{ g cm}^{-3}$  and clay fraction but is possibly only a smaller portion (Castellano et al., 2015) of physicochemically stabilized SOC.

The sentences that Laub and colleagues added should reflect that the actual correlation is with physicochemically stabilized SOC (mainly mineral-association) and not aggregated SOC. Conceptually it is unclear for me why aliphatic SOC should not be preferentially found in the mineral-associated fraction since this should be mainly microbial residues.

We agree that this statement was oversimplified and not correct as it was. From our perspective, chemical recalcitrance is mostly related to attractiveness for microbial consumption, as all complexities of carbon can eventually be decomposed (Kallenbach et al., 2016). The sentence was removed and a larger discussion added.

515 From a conceptual perspective DSI probably relates mainly to chemical recalcitrance of SOM present in different  
SOM fractions. In that respect it is different from physical light/heavy fraction separation approaches as each of  
these fractions is very heterogeneous. For examples, the light fraction has strong absorbance at both  
aliphatic saturated and aromatic/carboxylate unsaturated carbon bands (Calderón et al., 2011), so it could be that  
within each fraction, aliphatic saturated carbon is preferentially consumed by microorganisms. Thus, DSI reflects  
physicochemically stabilized SOC (mainly mineral-association in the case of bare soils) as also suggested by the  
520 correlation of the ratio of  $1620 \text{ cm}^{-1}/2930 \text{ cm}^{-1}$  absorption bands areas to the ratio of mineral associated  
carbon/light fraction carbon (Demyan et al. 2012). The relationship to mineral-association is in many models is  
represented by a texture adjustment factor. On the other hand, DSI does not directly relate to aggregated (i.e.  
occluded) SOM, and its applicability in models focusing on aggregation needs to be evaluated (i.e. by a separate  
spectral analysis of occluded and remaining fractions.

I would appreciate if the authors could discuss this a little bit more also in light of the results from  $^{13}\text{C}$ -NMR which would suggest that the light fraction is enriched in aromatics (lignin) and the heavy fraction fractions in aliphatics (microbial cell walls). I think it might be worthwhile to discuss this further when I am missing it also other readers might.

We agree that these are interesting points, but this could be highly site specific and depend on the soil and residue type. From what we found in the literature the light fraction is not only enriched in aromatics but contains a strong band from aliphatic compounds as well (Calderón et al., 2011). From our perspective, using  $^{13}\text{C}$ -NMR as a gold standard also has its drawbacks. The preparation requires completed demineralization of the soil, usually with HF acid. HF also destroys some of the SOM. Of course, it is then difficult to determine, which OM is destroyed. We hope that the paragraph we added to the discussion on this is to the liking of reviewer 2.

Apart from a more open discussion in this direction, I am happy with the changes made to the manuscript.

We are happy for this judgment of our article and would like to thank reviewer 2 for his constructive criticism during the review process of this paper. We think that the request for a more mechanistic understanding of the DSI helped to shape this article towards having a more process-oriented discussion.

Castellano, M.J., Mueller, K.E., Olk, D.C., Sawyer, J.E., Six, J., 2015. Integrating Plant Litter Quality, Soil Organic Matter Stabilization and the Carbon Saturation Concept. *Global Change Biology*.

Demyan, M.S., Rasche, F., Schulz, E., Breulmann, M., Müller, T., Cadisch, G., 2012. Use of specific peaks obtained by diffuse reflectance Fourier transform mid-infrared spectroscopy to study the composition of organic matter in a Haplic Chernozem. *63*, 189-199.

#### Reviewer 4:

In general I like the idea of your study, however, (i) several mistaken terms need to be corrected (“vibrational peaks of absorbance”, peaks instead of bands, “ratio of.. stretching vibrations”), (ii) the innovative aspect, and importance need to be clarified, and (iii) lots of details need to be clarified within material and methods (:most important is the DSI suggested to be a measure for SMB-C or SOM pools?). The paper need a careful revision (e.g. correction of mistakes terms, clarification of innovative aspect and importance, and addition of missing/ incomplete information in material and methods) before a complete review will be possible.

Some details:

There are some semantic mistakes:

a) the term “ratio of aliphatic C-H (2930 cm<sup>-1</sup>) to aromatic C=C (1620 cm<sup>-1</sup>) stretching vibrations” is not correct. According to textbooks on spectroscopy it should be called as a ratio between the area under aromatic and aliphatic absorption bands (which is also in accordance with the respective description in the materials and methods section in the manuscript under review.

Thank you for pointing out these terminology differences. We initially adapted the terms peak and peak area as is used in many publications (Egli et al., 2010; Pengerud et al., 2013; Stevenson, 1994; Yang, 2014). As this term seems to be suboptimal and is not used in specialized spectroscopy textbooks, we switched to the use of “area below absorption bands” as was suggested.

b) “vibrational peaks of absorbance (at L74 for example)”. Should be called absorption bands: Please note that if infrared light of a certain wavelength introduces a vibrations at molecular scale that light will loss intensity which is recorded in the (FTIR/DRIFT) spectra by respective signals. However, since that light is absorbed by the sample such signals are called absorption bands (not peaks since this term is in general used to describe much sharper signals (textbooks on spectroscopy). Mistaken terms like the ones mentioned above need to be corrected. Standard terms need to be used. An introduction of new (incorrect / mistaken) ones need to be avoided.

We adapted the suggested terminology throughout the text.

c) In the abstract the “ratio of aliphatic C-H (2930 cm<sup>-1</sup>) to aromatic C=C (1620 cm<sup>-1</sup>)” which means A1620 to A2930 ratio is mentioned as a measure for DSI, but according to equation (2) it is the ratio between (A1620) and (A1620 +A2930), THIS is different! Please revise the text accordingly throughout the whole manuscript.

Thanks for this comment, we understand that this formulation could be confusing. We need to distinguish between the original definition of the DSI (A1620/A2930, Demyan et al. 2012) and its corresponding use to partition SOM pools. We defined the DSI as the ratio of A2930/A1620 and set it to the ratio for SOM\_fast/SOM\_slow. Resulting from this, the fraction in the slow pool (analogous to the pool equation defined by Bruun and Jensen, 2002) is as the original equation: A1620/(A1620 +A2930). The fraction in the fast pool would be A2930/(A1620 +A2930). We have now both equations in the manuscript and added some text to explain this in detail.

turnover rates and 49 % in the slow pool for the Bruun et al. (2003) turnover rates (Table 2). For the DSI initialization, the ratio of the area below the saturated absorption bands to the area below the unsaturated absorption band was used as the ratio of SOM in the fast to SOM in the slow cycling SOM pool:

245 
$$\frac{\text{fast SOM}}{\text{slow SOM}} = \frac{A_{2930\text{cm}^{-1}}}{A_{1620\text{cm}^{-1}}} = DSI \quad (2)$$

Thus, analogous to Equation 1, the fraction of SOM in the slow pool was calculated with the formula

$$\text{slow SOM fraction} = \frac{A_{1620\text{cm}^{-1}}}{A_{1620\text{cm}^{-1}} + A_{2930\text{cm}^{-1}}} \quad (3)$$

250 With  $A_{2930\text{ cm}^{-1}}$  and  $A_{1620\text{ cm}^{-1}}$  being the specific peak-area of under the saturated and unsaturated carbon aliphatic and aromatic peaksband (described in section 2.1). The remaining carbon was allocated to the fast SOM

## Abstract

- should consist of short statements on introduction, problem of interest, objective, material and methods, results, discussion and the conclusion. However, the problem of interest is missing.

We rewrote the introduction of the abstract and now clearly state the problem of model initialization.

L25-26. Please clarify the meaning of: "DRIFTS stability index ....., was used to divide SOM into fast and slow cycling pools in the soil organic module of the DAISY model." How was this done? How could a ratio be used to divide different pools? It may be usable to reflect the RATIO between SLOW and FAST pool or the proportion.

We now explicitly wrote, that 2930/1620 was set equal to fast/slow SOM, see comment to c).

## Introduction

Clarify the innovative aspect and importance of your study.

We added two sentences to clarify.

1)

losses that were to up to 30 % of initial SOM. Hence there is a need for a reproducible proxy for SOM pool initialization to reduce the high uncertainty of SOM modelsinitiation.

2)

As a novel approach, this study uses information gained from DRIFTS spectra to partition measured SOM into pools of different complexity. DRIFTS can provide information on SOM quality, but also on texture and even

L73 Clarify the meaning of the sentence: "The interaction of mid-infrared energy with molecular bonds in soil produces typical vibrational peaks of absorbance at distinct wavelengths." It seems to be incomplete, refer to textbooks on FTIR/DRIFTS?

et al., 2015; Tinti et al., 2015). The interaction-absorbance of mid-infrared energy-light with by molecular bonds in the soil sample vibrating at the same frequency in soil produces typical vibrational peaks of absorbanceabsorption bands at distinct wavelengths (Stevenson, 1994). The area below absorption bands (in short

L74 note the term "vibrational peaks of absorbance" is wrong. Absorption bands results from vibrations at the molecular level, but they are called in any textbook as absorption bands. All statement like the one above need to be changed throughout the whole manuscript..

This was corrected throughout and addressed above in statement a)

L74 Clarify the meaning of the term “These”

We rewrote this section, see next comment.

L75 This is incorrect, the wavelength of the CH absorption band is related to vibrations of C-H bonds in the SOM but NOT to elements. Please correct the wording and CLARIFY THE MEANING:

~~absorbance~~ absorption bands at distinct wavelengths (Stevenson, 1994). The area below absorption bands (in short – band area), ~~se~~ can be linked to different molecular bonds of carbohydrates, nitrogenamides, silicates silicon and

L77 Stretching peak need to be corrected into absorption band throughout the whole manuscript.....

This was corrected and addressed above in statement a)

L75 to 80 please clarify and consider that this problem is already described by textbooks on spectroscopy but also by authors (e.g. Capriel 1997, Celi et al. 1997 among others) who interpret the CH absorption bond with respect to soil wettability. These authors already mentioned the overlap of CH bands by those of OH bands. BUT they also stated that the OH bands are not only present in water the OH is also part of SOM, and soil minerals (e.g. clay minerals, oxides, hydroxides, etc.). These OH band will remain in air dried soil samples as well in the ones dried at 37 to 105°C. But drying at higher temperature may affect the OH content of SOM and soil minerals thereby affecting the absorption bands in DRIFT/FTIR spectra (see Yeasmin, Reeves among others). Please correct this statement AND clarify how you ensure that the drying procedure did not affect the spectral properties of your samples. Add respective spectra into the supplement.

There is some evidence that the spectral properties of samples does not change after drying at 105°C (Duboc et al., 2016) as there were no significant differences between spectra of samples dried at different temperatures/methods when stored outside a desiccator. What we found, is that when drying at 105°C the 2930 cm<sup>-1</sup> band area has the best visibility as the surrounding OH band absorption is reduced. We observed that leaving samples outside the desiccator for several hours led to a regain of OH band absorption, but we did not specifically measure this effect, as this was not our focus. We used different drying temperatures for deriving the DSI for the initial test of the DSI because we were not sure, if high temperatures would have negative effects for the utility of the DSI for modelling. Spectra and more detailed explanation below.

L86 explain the background of the idea of SOM pool initialization.

This is explained in detail in the first paragraph of the introduction.

Material and Methods:

PLEASE describe in more detail the soil sampling. Which soils were taken where, at which time? Which is the year of establishment for each of the experiments, at which year did the bare-fallow started, and which are the sampling year(s)?

We added the season of sampling for Ultuna and Bad Lauchstädt, the frequency of measurements for the Kraichgau and Swabian Jura sites and wrote explicitly that experiment and bare fallow establishment were in the same years. For those interested in the exact sampling dates, we added the raw data of this study into the supplementary which includes dates of sampling.

L145 ff seem mostly belong to the discussion.

This detailed explanation of the integration process was added within the review process, as the clarification of this was a major request of the other reviewers.

How did you ensure that drying at 105°C did not result in artifacts? Add references different to your own work.

We tested the different temperatures to explore this issue. In our prior work (Laub et al., 2019) we found that there is a linear decrease with drying temperature of the broad OH band surrounding 2930  $\text{cm}^{-1}$ , which goes along with a linear increase of absorption bands area related to carbon, which mainly comes from a reduction of clay OH signal. This smooth trend with temperature does from our perspective not point towards artifacts. Still we were not sure, whether 105°C is the best representation of organic absorption bands, which is the reason why we tested different temperatures for modeling, respective SOM pool initializations. Our reasoning for the modelling was as follows: If drying produces artifacts, then model performance should be reduced, but it improved. We can also refer to the work of Duboc et al. (2016), who found no differences in ATR spectra between freeze drying, 60 °C and 105°C when samples were not stored in a desiccator. We attach example spectra of different drying temperatures as well as the (3x scaled) difference between the absorbance at 105°C and 32°C (32-105 °C) to illustrate the development of absorption bands. As can be seen, there is a gain of absorbance with higher drying temperatures for the most part of the spectra, while absorbance from the broad OH band is reduced (positive difference). From our perspective, drying at 105 °C therefore makes the SOM related bands better visible due to the removal of interfering OH. Additionally, using a combined in situ thermal DRIFTS and evolved gas technique (Demyan et al., 2013), soil samples were heated incrementally from 25 to 700 °C and either the evolved gas quantified or the mid-infrared spectrum of the soil itself was measured.  $\text{CO}_2$  evolution, which would imply combustion or off-gassing, was not found at temperatures up to 105 °C. As the overall goal is to get the best representation of SOM within the DRIFTS spectra, 105 °C seems the most appropriate drying temperature for our application.

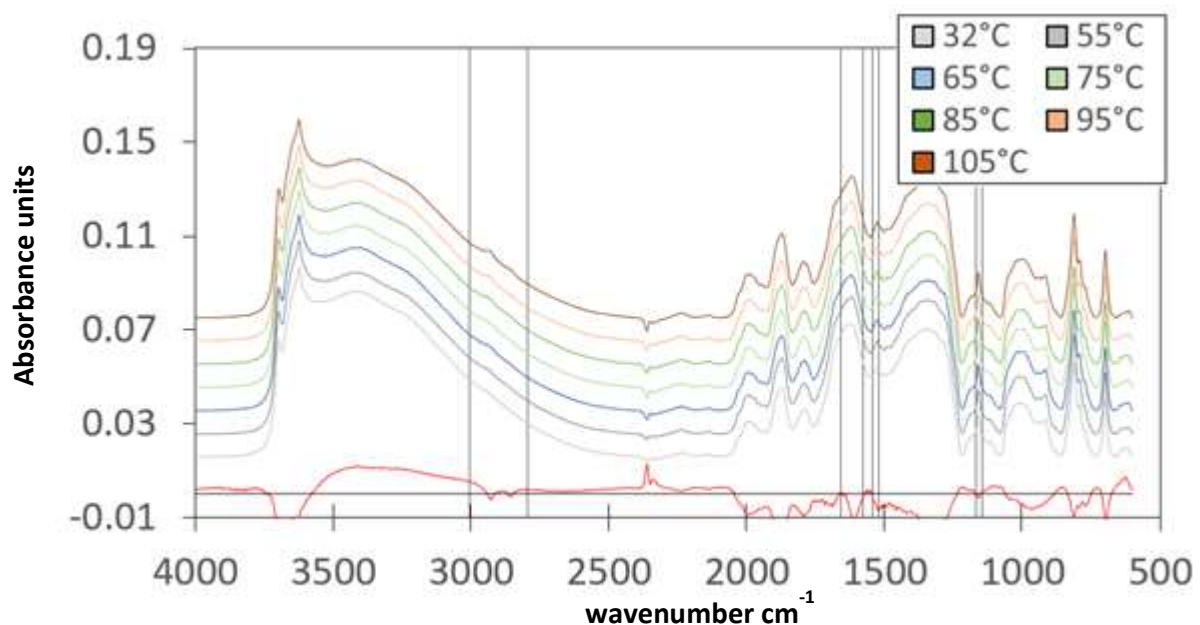


Figure 1 Baseline corrected example DRIFTS Spectra of bulk soil from the Swabian Jura (Table S1), dried at different temperatures. The red line indicates the difference of the 32 °C–105 °C absorbance (3× scaled for better illustration). The integration limits of the peak areas of interest are shown by vertical lines.



Add the limits of the band areas, how did you chose them?

The limits are stated (L143 of the prior version of the manuscript). They were initially chosen by Demyan et al. 2012; 2013, attempting to best resolve the 2930 and 1620  $\text{cm}^{-1}$  bands. This was based on isolated soil fractions, as well as spectra from substances rich in aromatic compounds, such as xylan and tannic acid. For the 2930  $\text{cm}^{-1}$  band, the range 3010-2800  $\text{cm}^{-1}$  was chosen as this avoids the aromatic C-H vibrations (if present) found around 3030  $\text{cm}^{-1}$  (Stevenson, 1994) and in soils investigated the 2930  $\text{cm}^{-1}$  aliphatic contribution (often a doublet on the very wide OH band) terminates at 2800  $\text{cm}^{-1}$ . For the 1620  $\text{cm}^{-1}$ , the limits of 1660-1580  $\text{cm}^{-1}$  were chosen as to include the anticipated range of aromatic C=C vibration variations while avoiding the amide band at <1580  $\text{cm}^{-1}$  and C=O of COOH and ketones at >1660  $\text{cm}^{-1}$  and significant mineral interference (e.g. Demyan et al., 2013) We fully recognize that including wavenumbers between 1630-1660  $\text{cm}^{-1}$  will probably also include C=O stretching of H-bonded C=O (Bellamy, 1975; Stevenson, 1994), thus have added in the manuscript (which was also cited in the Demyan et al., 2012 paper) that there is also a contribution of C=O within the band limits we use .

L171: meaning of the term “DAISY pools”? The ones mentioned in table 2 but table 2 show turnover rates, “maint” and “CUE”?

These additional parameters (maintenance respiration and carbon use efficiency) are explained in detail in Mueller et al. (1997). They are normal parameters in SOM models, but we did not alter them. We included them for completeness of the parameter set but decided for the main text to only include the relevant parameters that were changed and are relevant for the message, as readers can go back to original publications. We added a sentence to the caption of figure 2, to explain the difference between microbial turnover and death.

Describe the DSI evaluation, - initialization....

Those are described in chapter 2.3 and 2.4.

L194: Where is the description of SMB-C measurement? Please add a short s of SMB-C determination.

A description of SMB-C exists already at L 155 ff in the manuscript.

Please explain your reasons for dividing SMB-C into a fast and a slow cycling microbial pool. Why are they important?

This division is a default of DAISY. We added to the text, that we did a standard division, as this division is not the focus of this study.

According to the statements at L194 to 203 the SMB-C seemed to be assumed here as a measure for SOM. Is this correct, please explain! Please clarify the differences between the SMB-C pools (L194) and the SOM pools (L199)! AND CLARIFY which pool ratios will be described when using the  $A_{1620}/(A_{1620}+A_{2930})$  ratio?

We clarified in the text, that as bulk soil SOC included carbon from SMB-C, this needs to be subtracted from the amount of SOC that makes up the SOM pools carbon.

225 Measured bulk soil SOC includes SMB-C, therefore the amount of SOC in the fast and slow cycling SOM pools was bulk soil SOC minus SMB-C. As not focus of this study, a standard division of M<sub>measured</sub> SMB-C was divided into the slow and fast cycling microbial pools was done, with 10 % in the fast (8 % in Mueller et al., 1998) and 90 % in the slow pool. The remaining carbon (difference between total-bulk soil SOC and SMB-C) was divided between fast and slow cycling SOM pools either by either the DRIFTS stability index (DSI), or according to the

We also added a more detailed explanation of the DAISY pool to the section, where the models are explained.

and Linux systems. The DAISY model consists of two pools (fast and slow cycling) for each of the measurable fractions of 1) litter, 2) SMB and 3) stabilized SOM (Figure 1). Due to bare fallow, litter pools were disregarded in this study and the focus was on initializing the two SOM pools. A detailed description of the DAISY SOM

L405 please add background information for this statement (table, Fig.?, ref).

Did you consider somewhere in the discussion that the Bad Lauchstädt soil is a Chernozem? Please add missing information, old carbon present in Chernozem may cause difference in SOM turn-over (papers on black carbon etc...).

We added the reference to the figure 3, altered the text and added a new reference to this.

440 turnover rates. In the case of the Chernozem of Bad Lauchstädt, only turnover rates had an influence on model performance and. The its SOC turnover properties of the Chernozem were was generally not well captured overestimated with by either both parameter sets (Figure 3). It was previously suggested that the high SOC storage capacity of this site is related to a high content of adsorbed cations (Ellerbrock and Gerke, 2018)., and it probably has a slower overall SOM decomposition than many other agricultural soils. So a possible reason for an overestimation of SOC turnover in Bad Lauchstädt might be, that DAISY only considers clay content as stabilizing mechanism. Nevertheless, the use of DSI also was suitable for Bad Lauchstädt, as it did not reduce model

I stopped reading here since lots of information need to be clarified and added before a careful review will be possible.

We are grateful for the critical comments of the reviewer, who seems to be an expert in the field of SOM and soil spectroscopy. We think that addressing these, had further improved the quality of the manuscript.

Table 1 please add the studied sites, AND note SOC stand for SOIL organic carbon content please correct the capture accordingly refer to standard captures...

Explain the terms - UTM (abbreviation for ?), -“Depth of measurement” possibly the depth of sampling?, - the meaning of initial (SOC in soil in the year the bare fallow is established, of the SOC of soil in the year the experiment was established?)

Please add year of establishment and sampling; number of replicates

We added experiment name and reference for Ultuna and Bad Lauchstädt, year of establishment abbreviation of UTM, changed to depth of sampling and that fallow establishment and experiment establishment were at the same time.

Table 2 which of the pools are assumed to represent the fast/slow cycling SMB-C pools mentioned at L194?

We added additional explanation for the SMB pools which are subject to maintenance respiration and microbial death at the same time. We noticed that the SMB pool was wrongly named in figure 1 and changed this. The pools names are SMB and SOM – they contain C and N, but we did not focus on N simulation.

Table 3 show starting and ending year of the field experiment as well as ... SOC etc ... of the soil sampled at..... site. Please correct accordingly.

We added a longer heading, to explain the meaning of experiment start and simulation end etc. Correct the capture of table 4 and 5 accordingly...

We assessed and corrected the Table 4 and 5 once more.

Fig. 1 explain the meaning of the term "A\_XXXX"

Was done.

Fig. 2 I assume the capture should be: baseline corrected and vector normalized DRIFT spectra of 105°C dried soil samples from soils under bare fallow at ... site. Please indicate which figure shows what kind of spectrum. How did you ensure that drying at 105°C did not result in artifacts? If these spectra are baseline correct WHY did they start at different Y-axis values?

We changed the caption as requested. In the caption it is stated that the Y-axis offset was merely added for a better visibility. We added the size of offset (+0.02 for samples from the start).

References for the responses:

Bruun, S. and Jensen, L. S.: Initialisation of the soil organic matter pools of the Daisy model, *Ecol. Modell.*, 153(3), 291–295, doi:10.17665/1676-4285.20155108, 2002.

Calderón, F. J., Reeves, J. B., Collins, H. P. and Paul, E. A.: Chemical Differences in Soil Organic Matter Fractions Determined by Diffuse-Reflectance Mid-Infrared Spectroscopy, *Soil Sci. Soc. Am. J.*, 75(2), 568, doi:10.2136/sssaj2009.0375, 2011.

Demyan, M. S., Rasche, F., Schulz, E., Breulmann, M., Müller, T. and Cadisch, G.: Use of specific peaks obtained by diffuse reflectance Fourier transform mid-infrared spectroscopy to study the composition of organic matter in a Haplic Chernozem, *Eur. J. Soil Sci.*, 63(2), 189–199, doi:10.1111/j.1365-2389.2011.01420.x, 2012.

Demyan, M. S., Rasche, F., Schütt, M., Smirnova, N., Schulz, E. and Cadisch, G.: Combining a coupled FTIR-EGA system and in situ DRIFTS for studying soil organic matter in arable soils, *Biogeosciences*, 10(5), 2897–2913, doi:10.5194/bg-10-2897-2013, 2013.

Duboc, O., Tintner, J., Zehetner, F. and Smidt, E.: Does sample drying temperature affect the molecular characteristics of organic matter in soil and litter? A statistical proof using ATR infrared spectra, *Vib. Spectrosc.*, 85, 215–221, doi:10.1016/j.vibspec.2016.05.002, 2016.

Egli, M., Mavris, C., Mirabella, A. and Giaccai, D.: Soil organic matter formation along a chronosequence in the Morteratsch proglacial area (Upper Engadine, Switzerland), *CATENA*, 82(2), 61–69, doi:10.1016/j.catena.2010.05.001, 2010.

Kallenbach, C. M., Frey, S. D. and Grandy, A. S.: Direct evidence for microbial-derived soil organic matter formation and its ecophysiological controls, *Nat. Commun.*, 7, 1–10, doi:10.1038/ncomms13630, 2016.

Laub, M., Blagodatsky, S., Nkwain, Y. F. and Cadisch, G.: Soil sample drying temperature affects specific organic mid-DRIFTS peaks and quality indices, *Geoderma*, 355, 113897, doi:10.1016/j.geoderma.2019.113897, 2019.

Mueller, T., Jensen, L. S. S., Magid, J. and Nielsen, N. E. E.: Temporal variation of C and N turnover in soil after oilseed rape straw incorporation in the field: simulations with the soil-plant-atmosphere model DAISY, *Ecol. Modell.*, 99(2), 247–262, doi:http://dx.doi.org/10.1016/S0304-3800(97)01959-5, 1997.

Pengerud, A., Cécillon, L., Johnsen, L. K., Rasse, D. P. and Strand, L. T.: Permafrost Distribution Drives Soil Organic Matter Stability in a Subarctic Palsa Peatland, *Ecosystems*, 16(6), 934–947, doi:10.1007/s10021-013-9652-5, 2013.

Stevenson, F. J.: *Humus chemistry: genesis, composition, reactions*, John Wiley & Sons, New York., 1994.

Yang, X.: An extension to “Mid-infrared spectral interpretation of soils: Is it practical or accurate?,” *Geoderma*, 226–227(1), 415–417, doi:10.1016/j.geoderma.2014.03.022, 2014.

## DRIFTS peakband areas as measured pool size proxy to reduce parameter uncertainty of soil organic matter models

Moritz Laub<sup>1</sup>, Michael Scott Demyan<sup>2</sup>, Yvonne Funkuin Nkwain<sup>1</sup>, Sergey Blagodatsky<sup>1,3</sup>,  
Thomas Kätterer<sup>4</sup>, Hans-Peter Piepho<sup>5</sup>, Georg Cadisch<sup>1</sup>

5 <sup>1</sup> Institute of Agricultural Sciences in the Tropics (Hans-Ruthenberg-Institute), University of Hohenheim, 70599 Stuttgart, Garbenstrasse 13, Germany

<sup>2</sup> School of Environment and Natural Resources, The Ohio State University, Columbus, 2021 Coffey Rd., OH, USA, 43210

10 <sup>3</sup> Institute of Physicochemical and Biological Problems in Soil Science, Russian Academy of Sciences, 142290 Pushchino, Russia

<sup>4</sup> Department of Ecology, Swedish University of Agricultural Sciences, Uppsala, Ulls Väg 16, Sweden

<sup>5</sup> Institute of Biostatistics, University of Hohenheim, 70599 Stuttgart, Fruwirthstr. 23, Germany

15 *Correspondence to:* Moritz Laub ([moritz.laub@uni-hohenheim.de](mailto:moritz.laub@uni-hohenheim.de)) and Georg Cadisch ([Georg.cadisch@uni-hohenheim.de](mailto:Georg.cadisch@uni-hohenheim.de))

20 *Abbreviations:* ~~soil organic matter (SOM), Diffuse reflectance mid infrared Fourier transform spectroscopy (DRIFTS), DRIFTS stability index (DSI), equal wight (EW), original weight (OW), soil microbial biomass carbon (SMB-C), squared model error (SME), soil organic carbon (SOC), soil organic matter (SOM)~~

**Abstract.** [g1][ML2] ~~The initialization of soil organic matter (SOM) turnover models has been a challenge for decades. Soil organic matter (SOM) turnover models predict changes in SOM due to management and environmental factors. Their initialization remains challenging as partitioning of SOM into different hypothetical pools is intrinsically linked to model assumptions. Therefore, measurable pool partitioning proxies are needed. Diffuse reflectance mid infrared Fourier transform spectroscopy (DRIFTS) provides information on SOM quality and could yield a suitable for measureable pool partitioning proxy for SOM. This study tested DRIFTS derived SOM pool partitioning using the~~ Instead of using laborious and error-prone size-density fractionation for SOM pool partitioning, we propose a cost-effective, rapid, and non-destructive Diffuse reflectance mid-infrared Fourier transform spectroscopy (DRIFTS) technique on bulk soil samples to gain information on DAISY model. DRIFTS spectra were from SOM pool partitioning from infrared spectra bulk soil samples. Specifically, ~~the~~ DRIFTS stability index (DSI) of bulk soil samples was defined as the ratio of the area below the aliphatic absorption band C-H ( $2930\text{ cm}^{-1}$  [g3][ML4]) to the area below the aromatic/carboxylate absorption band aromatic C=C ( $1620\text{ cm}^{-1}$  [g5]) corresponding to C=O and aromatic C=C bonds stretching vibrations. For pool partitioning, the DSI (area ratio ~~short~~ =  $2930\text{ cm}^{-1}/1620\text{ cm}^{-1}$ ) was used set equal to the ratio of fast/slow cycling SOM. ~~to divide~~ SOM into fast and slow cycling pools in the soil organic module of the DAISY model. Performance was tested by ~~simulating~~ long-term bare fallow plots from the “Bad Lauchstädt extreme farmyard manure experiment” in

Germany (Chernozem, 25 years), the ~~and the~~ "Ultuna continuous soil organic matter field experiment" Ultuna  
frame trial in Sweden (Cambisol, 50 years) ~~were combined with~~ and 7 year duration bare fallow plots of 7 years  
40 ~~duration from the regions~~ Kraichgau and Swabian Jura ~~regions region~~ in Southwest Germany (Luvisols). ~~All fields~~  
~~All experiments had been in~~ were agricultural fields use for centuries before fallow establishment, so classical  
theory would suggest ~~an initial~~ that steady state can be assumed for initializing of SOM pools, ~~which was~~  
~~hence, enee~~ used to compare the performance of DAISY steady state and DSI initializations against the newly  
established DRIFTS stability index ~~initializations were compared, using in combination with~~. The test was done  
45 ~~using t~~ two different published parameter sets, ( $2.7 * 10^{-6} \text{ d}^{-1}$ ,  $1.4 * 10^{-4} \text{ d}^{-1}$ , 0.1 compared to  $4.3 * 10^{-5} \text{ d}^{-1}$ ,  
 $1.4 * 10^{-4} \text{ d}^{-1}$ , 0.3 for differing in the turnover rates slow and fast and ~~fast SOM pool turnover rates and~~  
humification efficiency, ~~respectively~~) were considered. The Initialization using DRIFTS DSI significantly  
initialization of SOM pools significantly reduced DAISY model error (for soil total soil organic carbon and  
microbial carbon) significantly for cases where assuming steady state led to had poor model performance. This  
50 was irrespective of the turnover rates used parameter set, but the faster turnover performed parameter set fitted  
better for all sites except for Bad Lauchstädt, ~~which~~ These results suggests that soils, although under long-term  
agricultural use, were not necessarily at steady state. In the next step, A Bayesian calibration was applied in a  
next step to identify inferred the best-fitting turnover rates for DAISY using the DRIFTS stability index DSI were  
evaluated either in DAISY, both for each each individual site individually and or for all sites combined a  
55 combination of all sites. The ~~t~~ two approaches which significantly reduced parameter uncertainty and  
equifinality in Bayesian calibrations were: 1) the adding of the physicochemical meaning with the DRIFTS  
stability index DSI (for for humification efficiency and slow SOM turnover), and 2) combining several all sites  
into one Bayesian calibration (for all parameters), as individual site derived turnover rates can be were strongly  
site specific. The The Bayesian calibration combining ation of all four sites showed suggested a potential for rapid  
60 that SOM loss is likely lost at relatively fast with turnover rates with the 95 % credibility intervals of for the slow  
SOM pools' the half-life of the slow SOM pools ranging from being 278 to 1095 years (with highest probability  
density at 426 years) as a value of highest probability density. The credibility intervals of this study were consistent  
with several recently published Bayesian calibrations of similar two-pool SOM models, i.e. all turnover rates being  
were considerably faster than earlier model calibrations suggested, hence those seed. It is therefore likely that they  
65 likely published turnover rates underestimated the potential SOM losses of SOM.

## 1 Introduction

Process-based models of plant-soil ecosystems are used from plot to global scales as tools of research and to  
support policy decisions (Campbell and Paustian, 2015). In soil organic matter (SOM) models, SOM is  
traditionally divided into several pools, representing fast and slow cycling or even inert SOM (Hansen et al., 1990;  
70 Parton et al., 1993). However, these theoretical SOM pools cannot easily be linked to measurable fractions. As a  
workaround, common methods of SOM pool initialization require that one assumes SOM at steady state  
conditions or includes a model spin-up run, ~~In a model spin-up run the user attemptings~~ to simulate SOM  
dynamics according to history and carbon inputs for the decades to several millennia prior to the period of actual  
interest (e.g. O'Leary et al., 2016). Theoretically if the SOM pools are at steady state and the turnover times of  
75 SOM pools are known, models can could be initialized, i.e. pool sizes calculated, either by simple equations (S-

Hansen et al., 2012)(e.g. for DAISY, Bruun and Jensen, 2002) or by inverse modeling (for RothC, Coleman and Jenkinson, 1996). In most cases, data is insufficient to guarantee that the assumptions of SOM steady state or long-term land use history and inputs are correct, given the lack of data of residue/manure input and weather variability for the required long-term timescales (> 200 years to millennia). Furthermore, exact turnover times of different SOM pools are unknown, which makes the results of inverse modelling and steady state initializations a direct result of model assumptions (Bruun and Jensen, 2002). Hence, while the approach should work in theory, the history of a site is usually not sufficiently known for the timescales that SOM needs to equilibrate. Therefore, the simulation of past carbon inputs and the assumption of steady state are a rough approximation at best. Hence, it is critical to find measurable proxies such as soil size density fractionation or infrared spectra (Sohi et al., 2001), that can provide information on the quality of SOM and help to disconnect the intrinsic link between turnover times and SOM pool division and hence help in SOM for SOM pool initialization (Sohi et al., 2001).

As was shown by Zimmermann et al. (2007), and recently confirmed by Herbst et al. (2018), a link exists between soil fractions obtained by size/density fractionation and fast and slow cycling SOM pools. However, Poeplau et al. (2013) showed, that the same fractionation protocol led to considerably different results at six different laboratories which regularly applied the technique (coefficient of variation from 14 to 138 %). The resulting differences in the model initializations for simulated SOM loss after 40 years of fallow, led to differences in SOM losses that were up to 30 % of initial SOM. Hence there is a need for a reproducible proxy for SOM pool initialization to reduce the high uncertainty of SOM model initiation.

We hypothesized that such a proxy could be obtained from inexpensive, high-throughput Diffuse Reflectance mid infrared Infrared Fourier transform Spectroscopy (DRIFTS).

As a novel approach, this study uses information gained from DRIFTS spectra to partition measured SOM into pools of different complexity. DRIFTS can provide information on SOM quality, but also on texture and even mineralogy (Nocita et al., 2015; Tinti et al., 2015). The interaction-absorbance of mid-infrared energy-light with by molecular bonds in the soil sample vibrating at the same frequency in soil produces typical vibrational peaks of absorbance-absorption bands at distinct wavelengths (Stevenson, 1994). The area below absorption bands (in short – band area), can be linked to different molecular bonds of carbohydrates, nitrogenamides, silicates silicon and other elements and others. The vibrational peaks which relate to carbon of different complexities, such as the aliphatic C-H stretching. Two important absorption bands peak that provide information on SOM quality are the aliphatic carbon band (in short 2930 cm<sup>-1</sup>, limits: around 2930-2800 cm<sup>-1</sup>) and the aromatic/carboxylate band (in short 1620 cm<sup>-1</sup>, limits: 1660 – 1580 cm<sup>-1</sup> – aromatic C=C stretching) peak at 1620 cm<sup>-1</sup>, provide information on SOM quality (Giacometti et al., 2013; Margenot et al., 2015; Pengerud et al., 2013). While both band peaks are subject to interference (2930 cm<sup>-1</sup> mainly from water and 1620 cm<sup>-1</sup> mainly from minerals (Nguyen et al., 1991)), it should be possible to limit the interference using subregions of the absorption peaks bands with carefully selected integration limits, only selecting the specific peak area of interest. Indeed, Demyan et al. (2012) found aliphatic-aliphatic compounds-carbon to be enriched under long-term farmyard manure application and depleted in mineral fertilizer or control treatments, and showed that the ratios of the 1620 cm<sup>-1</sup> to 2930 cm<sup>-1</sup> peak band area had a significant positive correlation with the ratio of stable to labile SOM obtained by size and density fractionation. It was further corroborated that the specific integration limits of the peaks band area they used, which

115 mainly selected the top subregion of the ~~peak areas~~ absorption bands, are ~~lost~~ strongly reduced or lost during  
combustion (Demyan et al., 2013). Hence, we hypothesized that the ratio of ~~areas below the aliphatic-aliphatic to~~  
~~aromatic-aromatic/carboxylate carbon~~ DRIFTS ~~peak~~ absorption bands ~~s~~ can be used as proxy for ~~the ratio of fast~~  
~~to slow cycling~~ SOM for pool initialization, thus providing a major improvement over assuming steady state SOM.  
120 ~~The~~is ratio ~~of areas below absorbance bands of aliphatic to aromatic/carboxylate of aliphatic to aromatic~~  
~~peak~~ carbon, will be referred to as the DRIFTS stability index (DSI) hereafter. Testing, improvement and proper  
use of the DSI was the central topic of this study. Recent findings have highlighted that the residual water content  
in bulk soil samples after drying at different temperatures affects the DSI considerably. Water absorbance affects  
significant parts of the mid-infrared spectra and particularly influences the 2930 and 1620 cm<sup>-1</sup> ~~peak~~ band areas  
(Laub et al., 2019). For this reason, we also tested how the drying temperature prior to DRIFTS measurements  
affects the use of the DSI proxy, using 32, 65 and 105°C as pretreatment temperatures.

125 To test our hypotheses about DSI performance, we used the DAISY SOM model (Hansen et al., 2012). DAISY is  
a commonly used SOM model (Campbell and Paustian, 2015) with a typical multi-pool structure, which includes  
two soil microbial biomass (~~SMB~~) pools, as well as two ~~pools for stabilized~~ SOM ~~pools~~ (fast and slow ~~cycling~~).  
With first-order turnover kinetics and a humification efficiency parameter (~~Figure 1~~ ~~Figure 1~~), the DAISY  
structure is similar to other widely used SOM models such as CENTURY (Parton et al., 1993) or ICBM (Andrén  
130 and Kätterer, 1997). Model SOM pool initialization using the DSI was compared to initialization via a steady state  
assumption with different published turnover rates. For this comparison bare fallow experiments from a range of  
different sites and time scales from one to five decades were included. Bare fallow experiments were used to avoid  
the added complexity caused by the conversion of different plant compounds into SOM of varying stabilities  
during decomposition.

135 As SOM pool sizes and turnover rates are closely linked, it could also be necessary to recalibrate DAISY  
parameters for the use of the DSI. Therefore, a Bayesian calibration of turnover rates was used to adjust DAISY  
turnover rates to the pool division and time dynamics of the measured DSI throughout the fallow period. Thus, the  
DAISY parameterization was evaluated with respect to equifinality and uncertainty as well as dependence on  
model structure. The final hypothesis was, that through a Bayesian calibration using the DSI, DAISY pools will  
140 correspond to measured, i.e. physiochemically meaningful fractions thus reducing uncertainty. The posterior  
credibility intervals and optima of turnover rates should correspond to the results of other Bayesian calibrations  
done for similarly structured two-pool models. If such relations could be confirmed, this would point towards  
fundamental insights about the intrinsic SOM turnover in temperate agroecosystems.

## 2 Material and Methods

### 145 2.1 Study sites and data used for modeling

Datasets originating from bare fallow treatments of four different sites with different experimental durations and  
measurement frequencies were used in this study. Topsoil (0-20 cm) samples were ~~available~~ received from the  
long-term experiments of (a) the ~~“Ultuna continuous soil organic matter field experiment”~~ ~~Ultuna~~ ~~Frame~~ trial  
(established in 1956, with additional ~~data~~ ~~samples~~ from 1979, 1995 and 2005; ~~samples always taken in autumn~~  
150 (Kätterer et al., 2011), four replicates), and (b) the Bad Lauchstädt ~~e~~Extreme ~~F~~farmyard ~~M~~manure ~~E~~experiment



(established in 1983, with additional ~~data samples~~ from 2001, 2004 and 2008 ~~samples always taken in autumn~~ (Blair et al., 2006), two replicates) (<https://www.ufz.de/index.php?de=37008>, date accessed 10.01.2019). Additional data ~~from two medium-term bare fallow experiments (established in autumn 2009 with data until 2016)~~ from Southwest German regions ~~were available~~ ~~was included~~. In these experiments ~~i.e. of (e) three fields in the region of (c) the Kraichgau and three fields in the region (d) the Swabian Jura, representing different climatic and geological conditions were intensely monitored.~~ The bare fallow plots (5 x 5 m size) in these ~~Southwest Germany~~ experiments were established within ~~the agricultural fields with three replicates per field~~ (Ali et al., 2015). ~~and Up to four topsoil samples (0-30 cm) were taken of top had monthly to yearly measurement frequencies of soil samples (0-30 cm) throughout the year per season were taken from 0-30 cm throughout the year in these.~~ In both regions, three replicates of bare fallow plots were established in each of three different fields. Further details on all the sites can be found in ~~Table 1~~ ~~Table 1~~. All sites had been under cultivation for at least several hundred years prior to establishing the bare fallow plots, which would suggest that steady state could be assumed.

~~All available b~~ Bulk soil samples ~~from the start and throughout the simulation period of all experiments~~ ~~Ultuna and Bad Lauchstädt~~ were analyzed for total organic carbon and DRIFTS spectra. ~~For Kraichgau and Swabian Jura sites, total organic carbon and DRIFTS spectra were only measured about once every two years, while ; samples from the Kraichgau and Swabian Jura sites were additionally analyzed for soil microbial biomass carbon (SMB-C) was measured up to four times per year. After sampling, a~~ All bulk soil samples (except for SMB-C) were passed through a 2 mm sieve, then air dried, ball milled (for two minutes) to powder and stored until further analysis. Soil organic carbon (SOC) content was analyzed with a Vario Max CNS (Elementar Analysensysteme GmbH, Hanau, Germany). Soil samples for DRIFTS analysis were obtained after 24-hr drying at 32, 65 and 105°C. The dried samples were kept in a desiccator until measurement. DRIFTS spectra of bulk soil samples (with four subsamples per sample) were obtained using an HTS-XT microplate extension, mounted to a Tensor-27 spectrometer using the processing software OPUS 7.5 (~~equipment and software from~~ Bruker Optik GmbH, Ettlingen, Germany). A potassium bromide (KBr) beam splitter with a nitrogen cooled HTS-XT reflection detector was used to record spectra in the mid infrared range (4000 – 400 cm<sup>-1</sup>). Each spectrum was a combination of 16 co-added scans with a 4 cm<sup>-1</sup> resolution. Spectra were recorded and then converted to absorbance units (AU); the acquisition mode “double-sided, forward-backward” and the apodization function Blackman-Harris-3 were used. After baseline correction and vector normalization of the spectra, ~~peak areas below absorptions bands~~ of interest were obtained by integration using a local baseline with the integration limits of Demyan et al. (2012). ~~and i~~ Integrated ~~peak band~~ areas of the four subsamples ~~were then~~ averaged. ~~after that~~ The local baselines were drawn between the intersection of the spectra and a vertical line at the integration limits (3010 – 2800 cm<sup>-1</sup> for the ~~aliphatic carbon band~~ ~~aliphatic C-H stretching~~, 1660 – 1580 cm<sup>-1</sup> for ~~aromatic C=C stretching vibrations~~ ~~the aromatic/carboxylate carbon band~~). Example spectra and integrated ~~bandpeak~~ areas are displayed in ~~Figure S 1~~ ~~Figure S 1~~. These ~~carefully selected~~ integration limits were ~~selected~~ ~~critical~~ ~~with the goal to reduce~~ ~~ing~~ signal interference from water and minerals, ~~using spectra of pure substances, clay minerals and from DRIFTS spectra gained during heating samples up to 700°C~~ (Demyan et al., 2013). Particularly, the mineral interference close to the 1620 cm<sup>-1</sup> ~~bandpeak~~ makes accurate selection of integration limits necessary, so that only its top part (assumed to consist mostly of ~~aromatic aromatic/carboxylate~~ carbon) is selected. In the case of our samples, the selected specific ~~bandpeak~~ area of the 1620 cm<sup>-1</sup> ~~bandpeak~~ accounted for approximately 10 to 30 % of the ~~total bandpeak~~ area ~~of the larger surrounding~~

190 band (Figure S 1, ca. 1755-1555 cm<sup>-1</sup>), and roughly integration limits were chosen so that the band area best  
corresponds to the peak portion that is lost with combustion or chemical oxidation (Demyan et al., 2013; Yeasmin  
et al., 2017). A strong correlation between the DSI and the percentage of centennially persistent SOC ( $r = 0.84$ )  
from the combined long term experiments used in this study (using values of centennially persistent SOC from  
Cécillon et al., 2018; and Franko and Merbach, 2017), showed that the DSI selected in this manner did in fact  
195 explain a large portion of the SOC quality change across sites (Figure S 2 Figure S 2).

Additionally, soils from the experiments in Kraichgau and Swabian Jura were analyzed for SMB-C using the  
chloroform fumigation extraction method (Joergensen and Mueller, 1996). Briefly, field moist samples were  
transported to the lab in a cooler, with extractions beginning within 24 hours after field sampling and the final  
SMB-C values corrected to an oven-dried (105° C) basis. The SMB-C was measured two to four times throughout  
200 the whole year. Stocks of SOC and SMB-C for 0-30 cm were calculated by multiplying the percentage of SOC  
and SMB-C with the bulk density and sampled layer thickness (Table 1 Table 1), respectively. Bulk density was  
assumed constant for Bad Lauchstädt, Kraichgau and Swabian Jura, while for Ultuna the initial 1.44 Mg m<sup>-3</sup>  
(Kirchmann et al., 2004) in the beginning was used for all but the last measurement, where 1.43 Mg m<sup>-3</sup> (Kätterer  
et al., 2011) was used. Due to low coarse fragment contents (< 5 % for Swabian Jura 3, < 2 % for Swabian Jura 1  
205 and < 1 % for the other six sites), and because changes in stone content throughout the simulation periods are  
unlikely, no correction for coarse fragment content was done.

## 2.2 Description of the simulation model: DAISY Expert-N 5.0

All simulations were conducted using the DAISY SOM model (Hansen et al., 2012) integrated into the Expert-N  
5.0 modeling framework. Expert-N 5.0 allows a wide range of soil, plant and water models to be combined and  
210 interchanged (Heinlein et al., 2017; Klein et al., 2017; Klein, 2018). Expert-N can be compiled both for Windows  
and Linux systems. The DAISY model consists of two pools (fast and slow cycling) for each of the measurable  
fractions of 1) litter, 2) SMB and 3) stabilized SOM (Figure 1). Due to bare fallow, litter pools were disregarded  
in this study and the focus was on initializing the two SOM pools. A detailed description of the DAISY SOM  
submodule as it was implemented into the Expert-N 5.0 framework can be found in Mueller et al. (1997). A  
215 graphical representation of the DAISY pools considered in this study is shown in Figure 1. The additional modules  
available for selection in the Expert-N 5.0 framework consist of a selection of established models for all simulated  
processes in the soil-plant continuum. The evaporation, ground heat, net radiation, and emissivity were simulated  
according to the Penman-Monteith equation (Monteith, 1976). Water flow through the soil profile was simulated  
by the Hydrus-flow module (van Genuchten, 1982) with the hydraulic functions according to Mualem (1976).  
220 Heat transfer through the soil profile was simulated with the DAISY heat module (Hansen et al., 1990). In the first  
step of the DSI evaluation, simulations were conducted with two established parameter sets for DAISY SOM. The  
first set was from Mueller et al. (1997) and was a modification of the original parameter set of turnover rates  
reported by Jensen et al. (1997). The second set was established after calibrations made by Bruun et al. (2003)  
using the Askov Long-Term Experiments, in which they introduced considerable changes to the turnover rates of  
225 the slow SOM pool and the humification efficiency. An equation developed by Bruun and Jensen (2002) was used  
to compute the proportions of the slow and fast cycling SOM pools for both parameter sets at steady state (see  
next section). Parameters of both sets are given in Table 2 Table 2.

For simulating soil temperature and moisture in Expert-N, daily averages of radiation, temperature, precipitation, relative humidity and wind speed are needed. For the long-term experiments they were extracted from the nearest weather station with complete data (Ultuna source: Swedish Agricultural University (SLU), ECA Station ID #5506, Elevation: 15 m, Lat: 59.8100 N, Long: 17.6500 E; Bad Lauchstädt source: Deutsche Wetter Dienst (DWD) Station #2932, Elevation: 131 m, Lat: 51.4348 N, Long: 12.2396 E, Locality name: Leipzig/Halle). For the fields of the Kraichgau and Swabian Jura, the driving variables were measured by weather stations installed next to eddy covariance stations located at the center of each field. Details on the measurements, instrumentation as well as gap filling methods of those eddy covariance weather stations are described in Wizemann et al. (2015).

### 2.3 SOM pool initializations with the DRIFTS stability index and at steady state

Measured bulk soil SOC includes SMB-C, therefore the amount of SOC in the fast and slow cycling SOM pools combined consists of bulk soil SOC minus measured SMB-C. As not focus of this study, Partitioning a standard division of M<sub>measured</sub> SMB-C was divided into the slow (90%) and fast (10%) cycling microbial pools was done similar to, with 10% in the fast (8% in Mueller et al., (1998) and 90% in the slow SMB pool.

The remaining carbon (difference between ~~total~~ bulk soil SOC and SMB-C) was divided between fast and slow cycling SOM pools either by either the DRIFTS stability index (DSI), or according to the steady state assumption. For ~~runs using a steady state assumption~~ division, the equation of Bruun and Jensen (2002) was used, which estimates the fraction of SOM in the slow pool at steady state from the model parameters under an assumed steady state:

$$\text{slow SOM fraction} = \frac{1}{1 + \frac{k_{SOM\_slow}}{f_{SOM\_slow} * k_{SOM\_fast}}} \quad (1)$$

with  $k_{SOM\_slow}$  and  $k_{SOM\_fast}$  representing the turnover (per day) of the slow and fast SOM pools respectively, and  $f_{SOM\_slow}$  representing the fraction of the fast SOM pool directed towards the slow SOM pool at turnover of fast SOM (humification efficiency). This resulted in 83 % of SOM being in the slow pool for the original DAISY turnover rates and 49 % in the slow pool for the Bruun et al. (2003) turnover rates (Table 2~~Table 2~~). For the DSI initialization, the ratio of the area below the aliphatic absorption bands to the area below the aromatic/carboxylate absorption band was used as the ratio of SOM in the fast to SOM in the slow cycling SOM pool:

$$\frac{\text{fast SOM}}{\text{slow SOM}} = \frac{A_{2930\text{cm}^{-1}}}{A_{1620\text{cm}^{-1}}} = DSI \quad (2)$$

Thus, analogous to Equation 1, the fraction of SOM in the slow pool was calculated with the formula

$$\text{slow SOM fraction} = \frac{A_{1620\text{cm}^{-1}}}{A_{1620\text{cm}^{-1}} + A_{2930\text{cm}^{-1}}} \quad (32)$$

With  $A_{2930\text{ cm}^{-1}}$  and  $A_{1620\text{ cm}^{-1}}$  being the specific peak area of under the aliphatic and aromatic/carboxylate aliphatic and aromatic peaksband (described in section 2.1). The remaining carbon was allocated to the fast SOM pool. As was mentioned before, three different data inputs for the DSI were used, obtained at drying temperatures of 32, 65 and 105°C, in order to test which drying temperature derived the best proxy for modeling. An example of the change of DRIFTS spectra occurring after several years of bare fallow can be found in Figure 2~~Figure 2~~.

All DSI model initializations were ~~then runsimulated~~ with both published sets of model parameters. Steady state initializations using **Equation 1** were only ~~conducted-simulated~~ with the corresponding parameter set from which they were calculated.

## 265 2.4 Statistical evaluation of model performance

Statistical analysis was performed with SAS version 9.4 (SAS Institute Inc., Cary, NC, USA). To compare different model initializations, a statistical analysis of squared model errors (SME) was conducted:

$$SME_x = (obs_x - pred_x)^2 \quad (43)$$

with  $obs_x$  being the observed value,  $pred_x$  the predicted value and  $x$  the simulated variable of interest. A linear mixed model with  $SME_x$  as response was then used to test for significant differences between initialization methods. This approach allowed us to make use of the statistical power of the three Kraichgau and Swabian Jura fields to analyze which initialization was most accurate and to evaluate the trend of the model error with increasing simulation time. In some cases,  $SME_x$  was transformed to ensure a normal distribution of residuals (square root transformation for Ultuna SOC and Kraichgau/Swabian Jura SMB-C and fourth root for Kraichgau/Swabian Jura SOC), which was checked by a visual inspection of the normal QQ plots and histograms of residuals (Kozak and Piepho, 2018). Random effects were included to account for temporal autocorrelation of  $SME_x$  within (a) the same field and (b) the same simulation. The model reads as follows:

$$y_{ijkl} = \phi_0 + \alpha_{0i} + \beta_{0j} + \gamma_{0ij} + \phi_1 t_k + \alpha_{1i} t_k + \beta_{1j} t_k + \gamma_{1ij} t_k + u_{kl} + u_{ijkl} \quad (54)$$

where  $y_{ijkl}$  is the  $SME_x$  of the simulation using the  $i$ th initialization with the  $j$ th parameter set, at the  $k$ th time on the  $l$ th field,  $\phi_0$  is an overall intercept,  $\alpha_{0i}$  is the main effect of the  $i$ th initialization,  $\beta_{0j}$  is the main effect  $j$ th parameter set,  $\gamma_{0ij}$  is the  $ij$ th interaction effect of initialization x parameter set,  $\phi_1$  is the slope of the time variable  $t_k$ ,  $\alpha_{1i} t_k$  is the interaction of the  $i$ th initialization with time,  $\beta_{1j} t_k$  is the interaction of the  $j$ th parameter set with time,  $\gamma_{1ij} t_k$  is the  $ij$ th interaction effect of initialization x parameter set x time,  $u_{kl}$  is the autocorrelated random deviation on the  $k$ th time in the  $l$ th field and  $u_{ijkl}$  is the autocorrelated residual error term corresponding to  $y_{ijkl}$ .

285 The detailed SAS code can be found in the supplementary material. For Ultuna and Bad Lauchstädt, the  $u_{kl}$  term was left out, as both trials only had one field. As the Kraichgau and Swabian Jura had the exact same experimental setup and duration, these sites were jointly analyzed in the statistic model, but due to completely different setups and durations, this was not possible for Bad Lauchstädt and Ultuna. The full models with all fixed effects were used to compare different correlation structures for the random effects including (i) temporal autocorrelation (exponential, spherical, Gaussian), (ii) compound symmetry, (iii) a simple random effect for each different field and simulation, (iv) a random intercept and slope of the time variable (with allowed covariance between both) for each field and initialization method. A residual maximum likelihood estimation of model parameters was used and the best fitting random effect structure for this model was selected using the Akaike Information Criterion as specified by Piepho et al. (2004). Then a stepwise model reduction was conducted until only the significant effects (290  $p < 0.05$ ) remained in the final statistical model. Because a mixed model was used, the Kenward-Roger method was applied for estimating the degrees of freedom (Piepho et al., 2004) and to compute post hoc Tukey-Kramer pairwise comparisons of means.

## 2.5 Model optimization and observation weighting for Bayesian calibration

Optimization of parameters  $k_{SOM\_slow}$ ,  $k_{SOM\_fast}$  and the humification efficiency ( $f_{SOM\_slow}$ ) was performed using a Bayesian calibration approach. These parameters were chosen as only they have a considerable impact on the rate of native SOM loss (see further details in the supplementary chapter S 12.2 ). The Bayesian calibration method uses an iterative process to simulate what the distribution of parameters would be, given the data and the model. It combines a random walk through the parameter space with a probabilistic approach on parameter selection.

The Differential Evolution Adaptive Metropolis algorithm (Vrugt, 2016) implemented in UCODE\_2014 (Lu et al., 2014; Poeter et al., 2014) was used for the Bayesian calibration in this study. As no Bayesian calibration of DAISY SOM parameters has been done before, noninformative priors were used. The main drawback of noninformative priors is that they can have longer computing times, but as was shown by Lu et al. (2012) with sufficient data and simulation durations, the posterior distributions are very similar to using informed priors. Ranges were set far beyond published parameters with  $1.4 * 10^{-2}$  to  $1.4 * 10^{-6} \text{ d}^{-1}$  for  $k_{SOM\_fast}$  and  $1.4 * 10^{-3}$  to  $5 * 10^{-7} \text{ d}^{-1}$  for  $k_{SOM\_slow}$ . The parameter  $f_{SOM\_slow}$  had to be more strongly constrained as without constraints it tended to run into unreasonable values up to 99 % humification. The limits were therefore set to 0.05 to 0.35, which is +/- 5 % of the two published parameter sets and represents the upper boundaries of other similar models (e.g. Ahrens et al., 2014). The default UCODE\_2014 Gelman-Rubin criterion (Gelman and Rubin, 1992) value of 1.2 was chosen for the convergence criteria. A total of 15 chains were run in parallel with a timestep of 0.09 days in Expert-N 5.0 (this was the largest timestep and fastest computation, where the simulation results of water flow, temperature and hence SOM pools was unaltered compared to smaller timesteps). It was ensured that at least 300 runs per chain were done after the convergence criterion was satisfied.

In Bayesian calibration, a proper weighing of observations is needed in order to achieve a diagonal weight matrix of residuals (proportional to the inverse of the variance covariance matrix), and to ensure that residuals are in the same units (Poeter et al., 2005, p18 ff). This included several steps. A differencing removed autocorrelation in the individual errors in each model run of the Bayesian calibration itself (the first measurement of each kind of data at each field was taken as raw data, for any repeated measurement the difference from this first measurement was taken instead of the raw data). Details on differencing are provided in chapter 3 of the UCODE\_2005 manual (Poeter et al., 2005). To account for varying levels of heterogeneity of different fields in the weighting, a mixed linear model was used to separate the variance of observations from different fields originating from natural field heterogeneity from the variance originating from measurement error. To do so, a linear mixed model with random slope and intercept of the time effect for each experimental plot was fitted to the SOC, SMB-C and DSI data for each field individually:

$$y_{kl} = \phi_0 + \phi_1 t_k + u_l + u_k + u_{kl} \quad (65)$$

where  $y_{kl}$  is the modeled variable at the  $k$ th time on the  $l$ th plot,  $\phi_0$  is the intercept,  $\phi_1$  is the slope of the time variable  $t_k$ ,  $u_l$  is the random intercept,  $u_k$  is the autocorrelated random deviation of the slope and  $u_{kl}$  is the autocorrelated residual error term corresponding to  $y_{kl}$ .

The error variance of each type of measurement (DSI, SMC-C, SOC) at each field  $\sigma_{fM}^2 = \sigma_{u_k}^2 + \sigma_{u_{kl}}^2$  was then used for weighting of observations, excluding the field variance  $\sigma_{u_l}^2$  from the weighting scheme. This error variance was used in UCODE\_2014 to compute weighted model residuals for each observation as follows:

$$w\_SME_x = \frac{(obs_x - pred_x)^2}{\sigma_{fM}^2} \quad (76)$$

where  $w\_SME_x$  is the weighted squared model residual,  $obs_x$  is the observed value,  $pred_x$  is the predicted value and  $\sigma_{fM}^2$  is the error variance of the  $M$ th type of measurement at each field. All  $w\_SME_x$  are combined to the sum of squared weighted residuals, which is the objective function used in UCODE\_2014 (Poeter et al., 2014). By this procedure, observations with higher measurement errors have a lower influence in the Bayesian calibration.

Since the medium-term experiments had a much higher measurement frequency, it was also tested if giving each experiment the same weight would improve the results of the Bayesian calibration (equal weight calibration). In this case an additional group weighting term was introduced for groups of observations, representing different datasets at the different sites. This weighting term is internally multiplied with each  $w\_SME_x$  in UCODE\_2014 and was calculated as

$$w\_G_x = \frac{1}{(n_{obs} * n_{par} * n_f)} \quad (87)$$

where  $w\_G_x$  is the weight multiplier for each observation,  $n_{obs}$  is the number of observations per parameter,  $n_{par}$  is the number of parameters per field, and  $n_f$  is the number of fields per site. This weighing assures that with the exact same percentage of errors, each site would have the exact weight of 1.

The influence of several factors was assessed in this Bayesian calibration: the use of individual sites compared to combining sites, including an equal weight (EW, as described above) vs original weight (OW) weighting only by error variance, and the effect of in/excluding the DSI (+/- DSI) in the Bayesian calibration. Therefore, seven Bayesian calibrations were conducted in total: four for each individual site with original weight and DSI, i.e., 1) Ultuna, 2) Bad Lauchstädt, 3) Kraichgau, 4) and Swabian Jura, 5) equal weight calibration for all sites combined using DSI, 6) original weight calibration for all sites combined without using DSI in the Bayesian calibration (only for initial pool partitioning) and 7) original weight calibration for all sites combined using the DSI. The comparison of these seven Bayesian calibrations was designed to assess the effect of the site on the calibration, as well as the effect of the DSI and of user weighting decisions.

### 3 Results

#### 3.1 Dynamics of SOC, SMB-C and DRIFTS during bare fallows

All bare fallow plots lost SOC over time with the severity of SOC loss varying between soils and climates at the different sites. The Bad Lauchstädt site experienced the slowest carbon loss (7% of initial SOC in 26 years), while SOC at Ultuna and Kraichgau was lost at much faster rates (Ultuna - 39% of initial SOC in 50 years, Kraichgau on average 9% of initial SOC in 7 years) (Table 3~~Table-3~~). In the Swabian Jura field 1 the SOC loss was comparable to that of Kraichgau (about 10% of initial SOC in 7 years), but was much less in fields 2 and 3. Some miscommunications with the field owner's contractors led to unwanted manure addition and fields ploughing in

Swabian Jura field 2 and 3 in 2013, hence results of these two fields after the incident in 2013 were excluded. The DRIFTS spectra revealed that the ~~aliphatic-aliphatic carbon bandpeak~~ area ( $2930\text{ cm}^{-1}$ ) decreased rather fast after the establishment of bare fallow plots while the ~~aromatic-aromatic/carboxylate bandpeak~~ area ( $1620\text{ cm}^{-1}$ ) ~~had~~ showed only minor changes and no consistent trend (**Figure 2**~~Figure-2~~). The ~~resulting-assumed~~ fraction of SOC in the slow SOM pool according to the ~~computed~~-DSI at  $105^{\circ}\text{C}$  changed from the initial range of 54 to 80 % to the range of 76 to 99% at the end of the observational period (**Table 3**, **Figure S 3**~~Figure-S-3~~). The SMB-C reacted even more rapidly to the establishment of fallows and halved on average for all fields within 7 years duration (**Table 3**).

### 3.2 Comparison of the different model initializations

The observed trend of SOC loss with ongoing bare fallow duration was also found in all simulations (**Figure 3**~~Figure-3~~ and **Figure S 4**~~Figure-S-4~~). For Ultuna, simulated SOC loss in all cases underestimated measured loss, while for Bad Lauchstädt, simulated SOC losses consistently overestimated measured losses. At Kraichgau sites SOC loss was underestimated by the models, ~~but~~ with the Bruun (2003) parameter set yielding simulated values closer to actual measurements. In the Swabian Jura, both parameter sets underestimated SOC loss. The decline of SMB-C in the Kraichgau and Swabian Jura (**Figure 4**~~Figure-4~~) occurred more rapidly than that of SOC, though SMB-C had higher variability of measurements. The parameter sets with steady state assumptions marked the upper and lower boundaries of the SMB-C simulations but the DRIFTS stability index (DSI) initializations were closer to the measured values (with exception of Swabian Jura field 3). For brevity only simulations of field 1 for Kraichgau and Swabian Jura are shown. Simulation results for fields 2 and 3 are found in the supplemental material (**Figure S 5**~~Figure-S-5~~ for SOC simulations and **Figure S 6**~~Figure-S-6~~ for SMB-C).

The statistical analysis of the model error revealed a site dependency of the effect of the parameter set. The three-way interaction of initialization, parameter set and time  $\gamma_{1ij}t_k$  was significant for all but Bad Lauchstädt SOC, where only the parameter set had a significant effect. In the case of Bad Lauchstädt, the model error was significantly lower with the slower Mueller (1997) SOM turnover parameter set, while for the rest of tested cases, the faster Bruun (2003) set performed significantly better (**Table 4**~~Table-4~~). For Ultuna and Kraichgau + Swabian Jura SOC, the steady state assumption with Mueller (1997) parameters had the highest model error, while the steady state assumption with Bruun (2003) parameters had the lowest model error of all simulations, ~~being similar to DSI initializations at Kraichgau and Swabian Jura. However, there was but there was only~~ a statistical significantly lower SOC model error with difference-of-DSI using  $105^{\circ}\text{C}$  drying temperature ~~compared than to the lower drying temperatures to DSI using other  $32^{\circ}\text{C}$  and  $65^{\circ}\text{C}$~~  for the Ultuna site. For SMB-C simulations at the Kraichgau + Swabian Jura sites, however, the errors were lowest for the DSI initialization using the  $105^{\circ}\text{C}$  drying temperature with Bruun (2003) parameters and significantly lower than both steady state initializations. Of the DSI initializations using different drying temperatures, the model error was always lowest when using the  $105^{\circ}\text{C}$  drying temperature initialization compared to  $32^{\circ}\text{C}$  and  $65^{\circ}\text{C}$  (significant for Ultuna, as well as for Kraichgau + Swabian Jura SMB-C using Mueller (1997) parameters). As initializations with DSI using  $105^{\circ}\text{C}$  drying temperature consistently performed best of all three DSI initializations, only DSI spectra of soils dried at  $105^{\circ}\text{C}$  were used for the Bayesian calibration.

### 3.3 Informed turnover rates of the Bayesian calibration

405 The posterior distribution of parameters from the Bayesian calibration differed considerably between the different calibrations for individual sites, but there were also differences between different weighting schemes or when performing the Bayesian calibration without using the DSI (**Figure 5**~~Figure 5~~). The highest probability turnover of the fast SOM pool ( $k_{SOM\_fast}$ ) was 1.5 and 3 times faster for Ultuna and Kraichgau, respectively, when compared to initial rates ( $1.4 * 10^{-4} \text{ d}^{-1}$  for both parameters sets), which fitted well for Bad Lauchstädt and Swabian Jura. For 410 the slow SOM pools ( $k_{SOM\_slow}$ ) the Bad Lauchstädt, Kraichgau and Swabian Jura site calibrations were in between the two published parameter sets, but tended towards the slower rates ( $2.7 * 10^{-6} \text{ d}^{-1}$  by Mueller (1997)), while the optimum for Ultuna was exactly at the fast rates of Bruun (2003) ( $4.3 * 10^{-5} \text{ d}^{-1}$ ). The humification efficiency ( $f_{SOM\_slow}$ ) was not strongly constrained in the Bayesian calibration, except for the Kraichgau site, where it ran into the upper boundary of 0.35. This trend towards higher humification existed also for the other sites, but to a lesser 415 extent than for Kraichgau.

The different calibrations of the combination of all sites under different weightings and with or without the DSI led to considerable differences in the posteriors (**Figure 5**) (~~Table 5~~g7). When combining the sites with the artificial equal weighting, the posterior distribution of all three parameters was the widest, basically covering the range of all four site calibrations. With the original weighting scheme, only informed by the variance of the data, 420 the posteriors were narrower for all parameters, with the optima of  $k_{SOM\_fast}$  being slightly faster than the two (similar) published rates. The optima of  $k_{SOM\_slow}$  were slightly slower than Bruun (2003) but much faster than Mueller (1997) and  $f_{SOM\_slow}$  was even above the higher Bruun (2003) value of 0.3. The use of the original weighting scheme without the use of the DSI in the Bayesian calibration did not constrain the  $f_{SOM\_slow}$  at all and had faster  $k_{SOM\_slow}$  and slower  $k_{SOM\_fast}$  than the one using the DSI. Both these Bayesian calibrations using the original 425 weighting (with and without DSI) showed a trend towards slightly faster turnover than suggested by Bruun (2003).

There was a strong negative correlation between  $k_{SOM\_fast}$  and  $k_{SOM\_slow}$  parameters for all but the Bad Lauchstädt calibration (**Figure S 7**~~Figure S 7~~). When DSI was not included in the Bayesian calibration, this negative correlation was stronger than when it was included (**Figure 6**~~Figure 6~~). The parameters  $k_{SOM\_fast}$  and  $f_{SOM\_slow}$  were always positively correlated, most strongly for Kraichgau (0.49) and Swabian Jura (0.38), but only weakly for the 430 long-term sites. The correlations between the parameters  $k_{SOM\_slow}$  and  $f_{SOM\_slow}$  were generally low and both positive and negative. The parameters with the highest probability density of the calibrations combining all sites for  $f_{SOM\_slow}$ ,  $k_{SOM\_fast}$  and  $k_{SOM\_slow}$  in that order were 0.34,  $2.29 * 10^{-4}$ ,  $3.25 * 10^{-5}$  for the original weight calibration and 0.06,  $9.58 * 10^{-5}$  and  $5.54 * 10^{-5}$  for the calibration using original weights and no DSI. These results suggest that turnover rates of  $k_{SOM\_slow}$  could be similar or faster than  $k_{SOM\_fast}$  without the use of the DSI. About 10 % of 435 simulations of the Bayesian calibration without DSI had even a faster  $k_{SOM\_slow}$  than  $k_{SOM\_fast}$ .

## 4 Discussion

### 4.1 How useful is the DRIFTS stability index?

A search for suitable proxies for SOM pool partitioning into SOM model pools that correspond to measurable and physicochemical meaningful quantities is of high interest (Abramoff et al., 2018; Bailey et al., 2018; Segoli et al., 440 2013). The results of this study confirm the hypothesized usefulness of the DSI proxy assessing the current state



of SOM for pool partitioning to model SOC for several soils across Europe. This is particularly relevant, given that changes in crop genotype and rotation, agricultural management, and the rise of average temperatures in recent decades as well as land use changes, such as draining of soils or deforestation, in recent centuries have altered the quality and quantity of carbon inputs to soil. Consequently, the steady state assumption for model initialization is not likely to be valid. Demyan et al. (2012) showed that with a careful selection of peak-integration limits for absorbance band areas, the DSI through identifying organic contributions in DRIFTS spectra is a sensitive indicator of SOM stability if mineralogy is similar (despite acknowledged mineral interference). Combined with a higher temperature (105 °C) for soil drying prior to DRIFTS analysis, a strong correlation between the portion of centennially persistent SOC and the DSI (Figure S 2~~Figure S 2~~) was found in our study which supports the hypothesis that ~~it~~ DSI might be of general applicability across sites. Results from modeling corroborated the usefulness of the DSI for SOM pool partitioning for soils of different properties across Europe. The statistical analysis of the model error for both SOC and SMB-C showed clearly that the DSI can improve poor model performance, especially ~~with~~ when the slower turnover rates of Mueller (1997) were used. When model performance is already satisfactory, the natural variability of the DSI can make model performance worse, as in the case of Ultuna SOC with Bruun (2003) parameters, but this reduction was minor compared to the improvement the DSI had over steady state assumptions at Ultuna with Mueller (1997) rates. The better results for Ultuna with the Bruun (2003) steady state might also just be an effect of turnover times still being too slow and hence the more SOC in the fast pool, the faster turnover is in general and the lower the model error. This was also indicated by faster optima by the Bayesian calibration compared to both published turnover rates. In the case of the Chernozem of Bad Lauchstädt, only turnover rates had an influence on model performance and, ~~The~~ its SOC turnover properties of the Chernozem were was generally not well captured overestimated with by either both parameter sets (Figure 3). It was previously suggested that the high SOC storage capacity of this site is a result of cation-bridging due to a high content of adsorbed cations (Ellerbrock and Gerke, 2018). Additionally, there is evidence for black carbon at the site (e.g. the high thermal stability found by (Demyan et al., 2013)., ~~and it probably has a slower overall SOM decomposition than many other agricultural soils. So~~ Therefore, a possible reason for an overestimation of SOC turnover in Bad Lauchstädt might be, that DAISY only considers clay content as a stabilizing mechanism. ~~Nevertheless, the use of DSI also was suitable for Bad Lauchstädt, as it did not reduce there was no significant difference in~~ model performance compared to steady state.

The range of different sites, soils, and climatic conditions of Europe represented within this study suggests the robustness of the DSI as a proxy for SOM quality and SOM pool division for a large environmental gradient. Hence, it would be an improvement over assuming steady state of SOM wherever there is a lack of detailed information of carbon inputs and climatic conditions. Considering the timescales at which SOM develops, this is almost anywhere, as detailed data is available at best for <200 years, which is not even one half-life of the slow SOM pool.

So far, studies that assessed SOM quality and pool division proxies, either using thermal stability of SOM (Cécillon et al., 2018) or size-density fractionation (Zimmermann et al., 2007), only indirectly related the proxies to inversely modeled SOM pool distributions, using machine learning and rank correlations. In contrast, our study showed that the DSI is a proxy which can be directly used for pool initialization. The DSI also makes sense from the perspective

of energy content, as microorganisms can obtain more energy from the breakdown of aliphatic than aromatic/carboxylate carbon ~~aliphatic than aromatic~~ compounds (e.g. Good and Smith, 1969), and therefore aliphatic-aliphatic carbon compounds are ~~is~~ primarily targeted by microorganisms (hence have faster turnover) as previously shown for bare fallows (Barré et al., 2016).

The two distinct peaks-absorption bands for aliphatic and aromatic/carboxylate ~~aliphatic and aromatic~~ carbon bonds of the DSI fit well to the two SOM pool structure of DAISY and the simulation of carbon flow through the soil in DAISY is very similar to several established SOM models such as SoilN, ICBM and CENTURY. It is therefore likely that with calibration, the DSI could be used as a general proxy for SOM models with two SOM pools and a humification efficiency ( $f_{SOM\_slow}$  in DAISY). The parameter correlations between  $k_{SOM\_slow}$ ,  $k_{SOM\_fast}$  and  $f_{SOM\_slow}$  according to the Bayesian calibrations also suggest that without a pool partitioning proxy, modifying any one parameter can lead to similar results in terms of SOC and SMB-C simulation. A clear distinction between fast and slow pools needs a pool partitioning proxy as can be seen by faster  $k_{SOM\_slow}$  than  $k_{SOM\_fast}$  for some of the simulations of the Bayesian calibration without using DSI. Assigning the DSI to DAISY reduced parameter correlations and led to a clear distinction between fast and slow SOM pools.

The aliphatic-molecular vibrational peak of DRIFTS absorption band for aliphatic carbon is most resolved when applying a 105°C drying temperature to samples prior to analysis (Laub et al., 2019). The current study's modeling results corroborated the finding that the DSI should be obtained from measurements after drying at 105 °C with the performance of the DRIFTS initializations being always in the order 105°C > 65°C > 32°C drying temperature (differences being sometimes but not always significant).

Compared with the other proxies for SOM quality discussed above, the measurements by DRIFTS are inexpensive, relatively simple, and the equipment of the same manufacturer is standardized. This should also constrain variability between different laboratories and be attractive for large-scale applications with large sample numbers, for example to initialize simulations at the regional scale. However, for standardization of the DSI for model initialization one needs to address how the type of spectrometer (e.g. detector type) influences the spectra, if water and mineral interferences (Nguyen et al., 1991) in the spectra can be further reduced and if a mathematical standardization of the spectra and DSI (across instruments and water contents) is possible. While a complete elimination of mineral interference is not possible, a careful selection of integration limits and the use of a local baseline minimizes mineral interference of DRIFTS spectra from bulk soils. This mostly selects the top part of the 1620 cm<sup>-1</sup> bandpeak area, which corresponds to the part that is reduced or completely lost when SOC is destroyed (Demyan et al., 2013; Yeasmin et al., 2017). Other approaches such as spectral subtraction of ashed samples or HF destruction of minerals prior DRIFTS analysis have been developed in the attempt to obtain spectra of pure SOC. All are rather labor intensive and still produce artifacts, as it is not possible to destroy only the minerals or only the SOC without altering the respective other fraction (Yeasmin et al., 2017). Hence, we think that the selected integration limits might represent at this point the most feasible option for obtaining a robust and cost-effective proxy of SOC quality for modeling. The strong correlation of DSI and centennially persistent SOC as well as the model results of this study seem to corroborate this. The method of DSI estimation might be improved by a study of the best integration limits optimizing the fit of the DSI and centennially persistent SOC, which would require more bare fallow experiments than in this study. ~~It could be worthwhile to use a~~ purely mineral peak [g8] ~~to correct~~

for the mineral interference at  $1620\text{ cm}^{-1}$  similar to what was done to correct for carbonates in the  $2930\text{ cm}^{-1}$  peak by Mirzaeitalarposhti et al. (2016).

520 From a conceptual perspective DSI probably relates mainly to chemical recalcitrance of SOM present in different SOM fractions. In that respect it is different from physical light/heavy fraction separation approaches as each of these fractions is very heterogeneous. For examples, the light fraction has strong absorbance at both aliphatic saturated and aromatic/carboxylate unsaturated carbon bands (Calderón et al., 2011), so it could be that within each fraction, aliphatic saturated carbon is preferentially consumed by microorganisms. Thus, DSI reflects physicochemically stabilized SOC (mainly mineral-association in the case of bare soils) as also suggested by the correlation of the ratio of  $1620\text{ cm}^{-1}/2930\text{ cm}^{-1}$  absorption bands to the ratio of mineral associated carbon/light fraction carbon (Demyan et al. 2012). The relationship to mineral-association is in many models is represented by a texture adjustment factor. On the other hand, DSI does not directly relate to aggregated (i.e. occluded) SOM, and its applicability in models focusing on aggregation needs to be evaluated (i.e. by a separate spectral analysis of occluded and remaining fractions.) [g9]

530 The recent coupling of pyrolysis with DRIFTS (Nkwain et al., 2018) might be a further analytical advancement of the DSI, as it overcomes mineral interferences in the spectra. However, this technique is more complex due to a larger number of visible organic absorption band peaks, including  $\text{CO}_2$  that develops from the pyrolysis, which makes it not easily applicable to established two-pool models such as DAISY. In addition, a considerable portion (30 – 40 %) of SOM is not pyrolyzed and therefore not recorded in the spectra. In summary, even despite of the acknowledged shortcomings, the DSI was useful to partition SOM between pools, even more so, when the optimized parameters for the DSI will be used for future applications. It seems more robust than steady state or long-term spin-up runs which rely on strong assumptions. Further tests are needed before using the DSI for mineralogy that differs considerably from the soils of this study. Finally, the DSI is not purely related to chemical recalcitrance of SOM, as it also correlates with the level of SOC protected by aggregation (Demyan et al., 2012). Hence, it is likely that aggregation and chemical recalcitrance are related.

#### 4.2 Parameter uncertainty as estimated with Bayesian calibration

545 According to our Bayesian calibrations, a wide range of parameter values are possible for DAISY going far beyond the initial published parameter sets. By combining various sites and including meaningful proxies, such as the DSI, the parameter uncertainty and equifinality could be reduced and the credibility intervals narrowed. The predictions of mechanistic models usually fail to account for the three main statistical uncertainties of (1) inputs, (2) scientific judgments resulting in different model setups and (3) driving data (Wattenbach et al., 2006). However, with a Bayesian calibration framework such as implemented in UCODE 2014, almost any model can be made probabilistic, so uncertainties of parameters and outputs can be assessed, even for projections into the future (Clifford et al., 2014). As this study focused on Bayesian calibration and we used an established model, we mainly address parameter uncertainty, although input uncertainty was also included through the weighting process. We clearly demonstrated an effect of the individual site used for Bayesian calibration on the resulting model parameters and uncertainties. Similarly diverging site specific turnover rates were also found by Ahrens et al.

(2014) in a study of soil carbon in forests. Diverging results for different sites generally point towards a need for a better understanding of the modeled system and model improvements (Poeter et al., 2005), but this often requires a deeper understanding of the system and new measurements – hence it is not always feasible. A Bayesian calibration asks the question: “What would be the probability distribution of parameters, given that the measured data should be represented by the selected model?”. Hence, if only one site is used, it can only answer this question for that specific site. As this study showed, the parameter set could then be highly biased for other sites. For a more robust calibration, several sites should be combined to obtain posterior distributions of parameters for a gradient of sites, though this might reduce model performance for individual sites. The introduction of the equal weighting scheme, which gave similar weights to the different sites, highlights how much bias may be introduced by user decisions of artificial weighting: this Bayesian calibration parameter set had the highest uncertainties and it appears as if the Ultuna site had by far the strongest influence. In contrast to that, the combination of all four sites with the original weights based on the error variances or measurements led to a very clear reduction of parameter uncertainty and the narrowest parameter credibility intervals (**Figure 6** **Figure-6 a** compared to **b** and **c**).

The results of the statistical analysis of model errors (**Table 4** **Table-4**) suggests that the DSI is suitable for **SOC model** pool initialization. This was corroborated by the Bayesian calibration, as the inclusion of the DSI narrowed credibility intervals for the slow SOM pool turnover and humification efficiency and reduced the correlation between fast and slow SOM turnover compared to the simulation without the DSI as constraint. Especially in the case of the clear differentiation between  $k_{SOM\_slow}$  and  $k_{SOM\_fast}$ , our results show the advantage of attaching a physiochemical meaning to the pools that was not provided before. Other effective approaches, such as time series of  $^{14}C$  data could be combined with the DSI for better results.

Of all three parameters, the humification efficiency ( $f_{SOM\_slow}$ ) was the only parameter that consistently ran into the upper boundaries, set to 35 %. In fact, initial calibrations were done where  $f_{SOM\_slow}$  was constrained to 95 %; even then, it tended to run into that constraint (**Figure S 8** **Figure-S-8**) and led to much faster turnover rates ( $k_{SOM\_slow}$ ) than were published before. These values of  $f_{SOM\_slow}$  were much greater than the 10 % for the Mueller (1997) dataset, 30 % for Bruun (2003), and other published two pool models. Therefore, we considered the cause of the poorly constrained  $f_{SOM\_slow}$  parameter was considered as being caused by to be a model formulation problem, which did not depend on whether the DSI was included in the Bayesian calibration or not. Only when the humification efficiency was restricted in the Bayesian calibration, the turnover of fast and slow SOM aligned with the earlier published rates. If a parameter is problematic, such as  $f_{SOM\_slow}$  it could mean that there is a lack of data. However, if parameters are constrained, but run into implausible values, it usually means that the model structure is suboptimal (Poeter et al., 2005) and should be altered.

### 4.3 Model structure determines SOM turnover times in two-pool models

The rate of SOM decomposition remains of major interest, especially with respect to the potential of SOM as a global carbon sink (Minasny et al., 2017). Some of the first conceptual approaches proposed SOM pools with residence times of 1000 years and longer (e.g. in CENTURY, Parton et al., 1987), but the SOM models were calibrated to fit data measured in long-term experiments that included vegetation. The pool structure of early SOM models such as DAISY and CENTURY were rather similar as were the turnover rates of SOM pools (see summary

in [Table 5Table-5](#)). An improved understanding of actual amounts of carbon inputs to the soil, which remain challenging to measure, led to faster turnover rates in more recent model versions (e.g. by Bruun, 2003). The reason is probably that inputs of carbon and nitrogen to the soil were initially underestimated as it is very difficult to measure root turnover and rhizosphere exudation inputs without expensive in situ <sup>13</sup>C or <sup>14</sup>C labeling. The underestimated inputs were then likely counterbalanced in the model calibration by slower turnover rates resulting in acceptable model outputs (SOM dynamics and CO<sub>2</sub> emissions) for the time being. However, as our summary of more recent studies underlines ([Table 5Table-5](#)), the earlier published turnover rates seem to be subject to a systematic underestimation. As the comparison of our Bayesian calibration to other recent Bayesian calibration studies suggests, the relatively fast turnover rates of this study are in alignment with other recent findings ([Table 5Table-5](#)), as all five examples have published turnover rates for the slow SOM pool, which are at least one order of magnitude faster than early assumptions from the 1980s and 90s.

It is critical to understand model uncertainties and to test fundamental assumptions of how SOM is transferred between the pools (Sulman et al., 2018). The comparison between constrained and unconstrained humification efficiency in the Bayesian calibrations suggests that the sequential flow of carbon through the system might be assuming a condensation of stabile carbon that does not actually explain the vast majority of more stable SOM formation. From a theoretical perspective, one may wonder how large amounts of less complex SOM should become complex SOM without any involvement of living soil organisms. The way that the formation of complex carbon is represented in DAISY is probably a remainder of earlier humification theories from the 1990s that mostly ignored microbe involvement, while most of the recent studies suggest that the vast majority of SOM is of microbial origin (Cotrufo et al., 2013). A simple adaption for two-pool SOM models such as DAISY that include SMB pools could acknowledge this paradigm shift: The partitioning between slow and fast turnover SOM could be at the death of the microbial biomass ([Figure 7Figure-7](#)) without any transfer of SOM from fast to slow pools (a brief test of this new structure is provided in the supplementary material [Figure S 10Figure-S-10](#)). This would also be in alignment with the DSI concept, as [aliphatic-aliphatic](#) carbon should not spontaneously transform to [aromatic-aromatic/carboxylate](#) carbon on its own. Then DAISY would fit better to the DSI and other proxies linking measurable fractions to SOM pools (the same is true for CENTURY and other models, which apply the same humification principle). The way that pools are linked in the current [setupmodel configuration, is such that](#) the actual turnover time of recalcitrant SOM consists of the turnover of the fast [pool](#) and ~~the~~ slow [SOM pools](#) combined as it moves through these pools sequentially ([Figure 1Figure-1](#)).

How strongly the basic [model](#) assumptions influence SOM simulations is also reflected when differences between one- and two-SOM pool models are compared. The turnover rates of the one-pool models are in between those of slow and fast [SOM](#) pools. However, our comparison shows that models with similar structure come to similar conclusions for SOM turnover. For example, the one-pool model in Clifford et al. (2014) was quite similar in turnover rates to that in Luo et al. (2016), but does not match well with two-pool models. Then again, the rates for the two-pool models of this study, and the studies by Ahrens et al. (2014) and Hararuk et al. (2017) were very similar in their minima and maxima, for both the slow and fast SOM pools, which shows that only models with a similar number of pools and transformations could be compared.

630 The 95 % credibility intervals of half-lives in DAISY were in the range from 278 to 1095 years for the slow SOM  
pool and from 47 to 90 years for the fast SOM pool for the combination of sites presented in this study. If these  
values were reasonable – and as the three recently published Bayesian calibrations including this study are quite  
close in turnover rates (Table 5Table 5), this seems to be the case, SOM could be lost at much faster rates under  
635 mismanagement and global warming than earlier modeling results suggest. The rates may also be biased towards  
an underestimation of turnover, as even with intense efforts it is next to impossible to keep bare fallow plots  
completely free of vegetation (weeds) and roots from neighboring plots. Recent studies are in alignment with the  
possibility of relatively fast SOC loss across various scales from field scale (Poyda et al., 2019) to country scale.  
For example in Germany, agricultural soils are much more often a carbon source than a sink (Jacobs et al., 2018).  
This highlights the importance of adequate SOM management and a deeper understanding of the processes at  
640 different scales. Especially in the context of understanding the response of SOM to climate change it is not enough  
if the SOM balance is simulated appropriately, but also fluxes within the plant-soil system need to be quantified.  
The reason is that under a warmer climate and changing soil moisture levels, the plant-derived carbon inputs will  
change. Furthermore, soil enzymatic analysis at regional and field level (Ali et al., 2015, 2018) suggest that pools  
of different complexity have different temperature sensitivities (Lefèvre et al., 2014), which is also realized in new  
models (Hararuk et al., 2017). If different pools have different responses to temperature, the formula by Bruun and  
645 Jensen (2002) for SOM pool distribution could not be used anymore, as it implicitly assumes a similar temperature  
sensitivity for all pools. In light of this, new proxies such as the DSI, soil fractionation or <sup>14</sup>C use (Menichetti et  
al., 2016), which could also be combined, are crucial for making SOM pools chemically or physically meaningful  
and to reduce model uncertainty and equifinality. As the DSI also had a good correlation with structurally protected  
SOM (Demyan et al., 2012) it could also fit very well to models that directly simulate the protection of SOM as a  
650 function of microbial activity (Sulman et al., 2014). A better understanding and the use of meaningful proxies such  
as DRIFTS, pyrolysis with DRIFTS (Nkwain et al., 2018) or thermal deconvolution (Cécillon et al., 2018; Demyan  
et al., 2013) in combination with Bayesian calibration and a wide range of long-term experiments are needed. The  
discrepancy between simulating SOM of tropical and temperate soils, which points towards a lack of understanding  
of fundamental difference in processes at work on the global scale would be the best test for future proxies and  
655 SOM models, which should be facilitated by freely available datasets for model testing and calibration.

## 5 Conclusion

We tested the use of the DRIFTS stability index as a proxy for initializing the two SOM pools in the DAISY model  
and used a Bayesian calibration to implement this proxy. A statistical analysis of model errors suggested that the  
660 use of DRIFTS stability index to initialize the fast and slow SOM pools significantly reduced model errors in  
most cases, especially those with initially poor performance. ~~It~~ DSI therefore seems to be a robust proxy to  
distinguish between fast and slow cycling SOM in order to initialize two-pool models and adds physicochemical  
meaning to the pools. As other studies have also shown, statistically sound approaches such as Bayesian calibration  
are needed to grasp the high uncertainty of SOM turnover, which is often neglected in modeling exercises. The  
665 results of the Bayesian optimization procedure further suggest that model performance could be improved by  
adjusting model parameters (turnover rates, humification efficiency) to the DSI initialization approach. Meaningful  
proxies such as DRIFTS, physical/chemical fractionation, or <sup>14</sup>C age assessments are likely to be the most robust

way to initialize SOM pools but their measurement method needs to be optimized to overcome known constraints, such as water and mineral interference in the case of DSI. The results of this study suggest that the turnover of SOM could be much faster than assumed by commonly used SOM models. For example, the DAISY slow SOM pool half-life estimated in our study ranged from 278 to 1095 years (95 % credibility intervals). The variability of parameters highlights the importance to include meaningful proxies into SOM models and to conduct research on a larger gradient of soils with bare fallow and planted sites, and over longer time frames.

## 6 Acknowledgements

This research was supported by the German Research Foundation (DFG) under the projects PAK 346 and the following FOR1695 “Agricultural Landscapes under Global Climate Change – Processes and Feedbacks on a Regional Scale” within subproject P3 (CA 598/6-1). We would like to thank Elke Schulz from the Department of Soil Ecology, Helmholtz Centre for Environmental Research in Halle/Saale for the provision of samples from Bad Lauchstädt. We would also like to thank Steffen Mehl, from the UCODE development team, for his help with the weighing of observations and the troubleshooting during the setup of UCODE\_2014 on the bWUniCluster. Finally, we thank the editor and all reviewers, especially Lauric Cécillon for the fruitful discussions during the review process. The authors acknowledge support by the state of Baden-Württemberg through bwHPC.

## 7 Data availability

Data of SOC from Ultuna and Bad Lauchstädt have already been published in the last decades and are cited in the text. The data of Kraichgau and Swabian Jura has not been published yet, but is provided in the graphs. ~~All measurements of DRIFTS are unpublished to this point. We are happy to make the full dataset publicly available, once accepted for publication.~~ The raw data which was used in this study is available in the supplement of this [article](#).

## 8 References

- Abramoff, R., Xu, X., Hartman, M., O'Brien, S., Feng, W., Davidson, E., Finzi, A., Moorhead, D., Schimel, J., Torn, M. and Mayes, M. A.: The Millennial model: in search of measurable pools and transformations for modeling soil carbon in the new century, *Biogeochemistry*, 137(1–2), 51–71, doi:10.1007/s10533-017-0409-7, 2018.
- Ahrens, B., Reichstein, M., Borken, W., Muhr, J., Trumbore, S. E. and Wutzler, T.: Bayesian calibration of a soil organic carbon model using  $\Delta^{14}\text{C}$  measurements of soil organic carbon and heterotrophic respiration as joint constraints, *Biogeosciences*, 11(8), 2147–2168, doi:10.5194/bg-11-2147-2014, 2014.
- Ali, R. S., Ingwersen, J., Demyan, M. S., Funkuin, Y. N., Wizemann, H.-D., Kandeler, E. and Poll, C.: Modelling in situ activities of enzymes as a tool to explain seasonal variation of soil respiration from agro-ecosystems, *Soil Biol. Biochem.*, 81, 291–303, doi:10.1016/j.soilbio.2014.12.001, 2015.
- Ali, R. S., Kandeler, E., Marhan, S., Demyan, M. S., Ingwersen, J., Mirzaeitalarposhti, R., Rasche, F., Cadisch, G. and

- Poll, C.: Controls on microbially regulated soil organic carbon decomposition at the regional scale, *Soil Biol. Biochem.*, 118(December 2017), 59–68, doi:10.1016/j.soilbio.2017.12.007, 2018.
- Andr n, O. and K tterer, T.: ICBM: The introductory carbon balance model for exploration of soil carbon balances, *Ecol. Appl.*, 7(4), 1226–1236, doi:10.1890/1051-0761(1997)007[1226:ITICBM]2.0.CO;2, 1997.
- 705 Bailey, V. L., Bond-Lamberty, B., DeAngelis, K., Grandy, A. S., Hawkes, C. V., Heckman, K., Lajtha, K., Phillips, R. P., Sulman, B. N., Todd-Brown, K. E. O. and Wallenstein, M. D.: Soil carbon cycling proxies: Understanding their critical role in predicting climate change feedbacks, *Glob. Chang. Biol.*, 24(3), 895–905, doi:10.1111/gcb.13926, 2018.
- 710 Barr , P., Plante, A. F., C cillon, L., Lutfalla, S., Baudin, F., Bernard, S., Christensen, B. T., Eglin, T., Fernandez, J. M., Houot, S., K tterer, T., Le Guillou, C., Macdonald, A., van Oort, F. and Chenu, C.: The energetic and chemical signatures of persistent soil organic matter, *Biogeochemistry*, 130(1–2), 1–12, doi:10.1007/s10533-016-0246-0, 2016.
- 715 Blair, N., Faulkner, R. D., Till, A. R., Korschens, M. and Schulz, E.: Long-term management impacts on soil C, N and physical fertility. Part II: Bad Lauchstadt static and extreme FYM experiments, *Soil Tillage Res.*, 91(1–2), 39–47, doi:10.1016/j.still.2005.11.001, 2006.
- Bruun, S. and Jensen, L. S.: Initialisation of the soil organic matter pools of the Daisy model, *Ecol. Modell.*, 153(3), 291–295, doi:10.17665/1676-4285.20155108, 2002.
- 720 Bruun, S., Christensen, B. T., Hansen, E. M., Magid, J. and Jensen, L. S.: Calibration and validation of the soil organic matter dynamics of the Daisy model with data from the Askov long-term experiments, *Soil Biol. Biochem.*, 35(1), 67–76, doi:10.1016/S0038-0717(02)00237-7, 2003.
- Calder n, F. J., Reeves, J. B., Collins, H. P. and Paul, E. A.: Chemical Differences in Soil Organic Matter Fractions Determined by Diffuse-Reflectance Mid-Infrared Spectroscopy, *Soil Sci. Soc. Am. J.*, 75(2), 568, doi:10.2136/sssaj2009.0375, 2011.
- 725 Campbell, E. E. E. and Paustian, K.: Current developments in soil organic matter modeling and the expansion of model applications: a review, *Environ. Res. Lett.*, 10(12), 123004, doi:10.1088/1748-9326/10/12/123004, 2015.
- C cillon, L., Baudin, F., Chenu, C., Houot, S., Jolivet, R., K tterer, T., Lutfalla, S., Macdonald, A., van Oort, F., Plante, A. F., Savignac, F., Souc mariadin, L. N. and Barr , P.: A model based on Rock-Eval thermal analysis to quantify the size of the centennially persistent organic carbon pool in temperate soils, *Biogeosciences*, 15(9), 2835–2849, doi:10.5194/bg-15-2835-2018, 2018.
- 730 Clifford, D., Pagendam, D., Baldock, J., Cressie, N., Farquharson, R., Farrell, M., Macdonald, L. and Murray, L.: Rethinking soil carbon modelling: a stochastic approach to quantify uncertainties, *Environmetrics*, 25(4), 265–278, doi:10.1002/env.2271, 2014.
- Coleman, K. and Jenkinson, D. S.: RothC-26.3 - A Model for the turnover of carbon in soil, in *Evaluation of Soil Organic Matter Models*, pp. 237–246, Springer Berlin Heidelberg, Berlin, Heidelberg., 1996.
- 735 Cotrufo, M. F., Wallenstein, M. D., Boot, C. M., Deneff, K. and Paul, E.: The Microbial Efficiency-Matrix Stabilization (MEMS) framework integrates plant litter decomposition with soil organic matter stabilization: do labile plant inputs form stable soil organic matter?, *Glob. Chang. Biol.*, 19(4), 988–995, doi:10.1111/gcb.12113, 2013.
- 740 Demyan, M. S., Rasche, F., Schulz, E., Breulmann, M., M ller, T. and Cadisch, G.: Use of specific peaks obtained by diffuse reflectance Fourier transform mid-infrared spectroscopy to study the composition of organic matter in a Haplic Chernozem, *Eur. J. Soil Sci.*, 63(2), 189–199, doi:10.1111/j.1365-2389.2011.01420.x, 2012.
- Demyan, M. S., Rasche, F., Sch tt, M., Smirnova, N., Schulz, E. and Cadisch, G.: Combining a coupled FTIR-EGA system and in situ DRIFTS for studying soil organic matter in arable soils, *Biogeosciences*, 10(5), 2897–2913, doi:10.5194/bg-10-2897-2013, 2013.
- 745 Ellerbrock, R. H. and Gerke, H. H.: Explaining soil organic matter composition based on associations between OM and polyvalent cations, *J. Plant Nutr. Soil Sci.*, 181(5), 721–736, doi:10.1002/jpln.201800093, 2018.



- Franko, U. and Merbach, I.: Modelling soil organic matter dynamics on a bare fallow Chernozem soil in Central Germany, *Geoderma*, 303(May), 93–98, doi:10.1016/j.geoderma.2017.05.013, 2017.
- Gelman, A. and Rubin, D. B.: Inference from Iterative Simulation Using Multiple Sequences, *Stat. Sci.*, 7(4), 457–472, doi:10.1214/ss/1177011136, 1992.
- 750 van Genuchten, M. T.: A comparison of numerical solutions of the one-dimensional unsaturated—saturated flow and mass transport equations, *Adv. Water Resour.*, 5(1), 47–55, doi:10.1016/0309-1708(82)90028-8, 1982.
- Giacometti, C., Demyan, M. S., Cavani, L., Marzadori, C., Ciavatta, C. and Kandeler, E.: Chemical and microbiological soil quality indicators and their potential to differentiate fertilization regimes in temperate agroecosystems, *Appl. Soil Ecol.*, 64, 32–48, doi:10.1016/j.apsoil.2012.10.002, 2013.
- 755 Good, W. D. and Smith, N. K.: Enthalpies of combustion of toluene, benzene, cyclohexane, cyclohexene, methylcyclopentane, 1-methylcyclopentene, and n-hexane, *J. Chem. Eng. Data*, 14(1), 102–106, doi:10.1021/jc60040a036, 1969.
- Hansen, S., Jensen, L. S., Nielsen, N. E. and Svendsen, H.: *DAISY - Soil Plant Atmosphere System Model*, Copenhagen: The Royal Veterinary and Agricultural University., 1990.
- 760 Hararuk, O., Shaw, C. and Kurz, W. A.: Constraining the organic matter decay parameters in the CBM-CFS3 using Canadian National Forest Inventory data and a Bayesian inversion technique, *Ecol. Modell.*, 364, 1–12, doi:10.1016/j.ecolmodel.2017.09.008, 2017.
- Heinlein, F., Biernath, C., Klein, C., Thieme, C. and Priesack, E.: Evaluation of Simulated Transpiration from Maize Plants on Lysimeters, *Vadose Zo. J.*, 16(1), 0, doi:10.2136/vzj2016.05.0042, 2017.
- 765 Herbst, M., Welp, G., Macdonald, A., Jate, M., Hädicke, A., Scherer, H., Gaiser, T., Herrmann, F., Amelung, W. and Vanderborght, J.: Correspondence of measured soil carbon fractions and RothC pools for equilibrium and non-equilibrium states, *Geoderma*, 314(November 2017), 37–46, doi:10.1016/j.geoderma.2017.10.047, 2018.
- Jacobs, A., Flessa, H., Don, A., Heidkamp, A., Prietz, R., Dechow, R., Gensior, A., Poeplau, C., Riggers, C., Schneider, F., Tiemeyer, B., Vos, C., Wittnebel, M., Müller, T., Säurich, A., Fahrion-Nitschke, A., Gebbert, S., Hopfstock, R., Jaconi, A., Kolata, H., Lorbeer, M., Schröder, J., Laggner, A., Weiser, C. and Freibauer, A.: *Landwirtschaftlich genutzte Böden in Deutschland – Ergebnisse der Bodenzustandserhebung - Thünen Report 64*, Johann Heinrich von Thünen-Institut, Bundesallee 50, 38116 Braunschweig, Germany., 2018.
- 770 Jensen, L. S., Mueller, T., Nielsen, N. E., Hansen, S., Crocker, G. J., Grace, P. R., Klír, J., Körschens, M. and Poulton, P. R.: Simulating trends in soil organic carbon in long-term experiments using the soil-plant-atmosphere model DAISY, *Geoderma*, 81(1), 5–28, doi:http://dx.doi.org/10.1016/S0016-7061(97)88181-5, 1997.
- Joergensen, R. G. and Mueller, T.: The fumigation-extraction method to estimate soil microbial biomass: Calibration of the kEC value, *Soil Biol. Biochem.*, 28(1), 25–31, doi:10.1016/0038-0717(95)00102-6, 1996.
- 780 Kätterer, T., Bolinder, M. A., Andrén, O., Kirchmann, H. and Menichetti, L.: Roots contribute more to refractory soil organic matter than above-ground crop residues, as revealed by a long-term field experiment, *Agric. Ecosyst. Environ.*, 141(1–2), 184–192, doi:10.1016/j.agee.2011.02.029, 2011.
- Kirchmann, H., Haberhauer, G., Kandeler, E., Sessitsch, A. and Gerzabek, M. H.: Effects of level and quality of organic matter input on carbon storage and biological activity in soil: Synthesis of a long-term experiment, *Global Biogeochem. Cycles*, 18(4), n/a-n/a, doi:10.1029/2003GB002204, 2004.
- 785 Klein, C., Biernath, C., Heinlein, F., Thieme, C., Gilgen, A. K., Zeeman, M. and Priesack, E.: Vegetation Growth Models Improve Surface Layer Flux Simulations of a Temperate Grassland, *Vadose Zo. J.*, 16(13), 0, doi:10.2136/vzj2017.03.0052, 2017.
- Klein, C. G.: *Modeling fluxes of energy and water between land surface and atmosphere for grass- and cropland system*, Fakultät Wissenschaftszentrum Weihenstephan., 2018.
- 790 Kozak, M. and Piepho, H. P.: What’s normal anyway? Residual plots are more telling than significance tests when checking ANOVA assumptions, *J. Agron. Crop Sci.*, 204(1), 86–98, doi:10.1111/jac.12220, 2018.

- Laub, M., Blagodatsky, S., Nkwain, Y. F. and Cadisch, G.: Soil sample drying temperature affects specific organic mid-DRIFTS peaks and quality indices, *Geoderma*, 355, 113897, doi:10.1016/j.geoderma.2019.113897, 2019.
- 795 Lefèvre, R., Barré, P., Moyano, F. E., Christensen, B. T., Bardoux, G., Eglin, T., Girardin, C., Houot, S., Kätterer, T., van Oort, F. and Chenu, C.: Higher temperature sensitivity for stable than for labile soil organic carbon - Evidence from incubations of long-term bare fallow soils, *Glob. Chang. Biol.*, 20(2), 633–640, doi:10.1111/gcb.12402, 2014.
- Lu, D., Ye, M. and Hill, M. C.: Analysis of regression confidence intervals and Bayesian credible intervals for uncertainty quantification, *Water Resour. Res.*, 48(9), 1–20, doi:10.1029/2011WR011289, 2012.
- 800 Lu, D., Ye, M., Hill, M. C., Poeter, E. P. and Curtis, G. P.: A computer program for uncertainty analysis integrating regression and Bayesian methods, *Environ. Model. Softw.*, 60(October), 45–56, doi:10.1016/j.envsoft.2014.06.002, 2014.
- Luo, Z., Wang, E., Shao, Q., Conyers, M. K. and Liu, D. L.: Confidence in soil carbon predictions undermined by the uncertainties in observations and model parameterisation, *Environ. Model. Softw.*, 80, 26–32, doi:10.1016/j.envsoft.2016.02.013, 2016.
- 805 Margenot, A. J., Calderón, F. J., Bowles, T. M., Parikh, S. J. and Jackson, L. E.: Soil Organic Matter Functional Group Composition in Relation to Organic Carbon, Nitrogen, and Phosphorus Fractions in Organically Managed Tomato Fields, *Soil Sci. Soc. Am. J.*, 79(3), 772, doi:10.2136/sssaj2015.02.0070, 2015.
- Menichetti, L., Kätterer, T. and Leifeld, J.: Parametrization consequences of constraining soil organic matter models by total carbon and radiocarbon using long-term field data, *Biogeosciences*, 13(10), 3003–3019, doi:10.5194/bg-13-3003-2016, 2016.
- 810 Minasny, B., Malone, B. P., McBratney, A. B., Angers, D. A., Arrouays, D., Chambers, A., Chaplot, V., Chen, Z.-S., Cheng, K., Das, B. S., Field, D. J., Gimona, A., Hedley, C. B., Hong, S. Y., Mandal, B., Marchant, B. P., Martin, M., McConkey, B. G., Mulder, V. L., O'Rourke, S., Richer-de-Forges, A. C., Odeh, I., Padarian, J., Paustian, K., Pan, G., Poggio, L., Savin, I., Stolbovov, V., Stockmann, U., Sulaeman, Y., Tsui, C.-C., Vågen, T.-G., van Wesemael, B. and Winowiecki, L.: Soil carbon 4 per mille, *Geoderma*, 292, 59–86, doi:10.1016/j.geoderma.2017.01.002, 2017.
- 815 Mirzaeitalarposhti, R., Demyan, M. S., Rasche, F., Cadisch, G. and Müller, T.: Overcoming carbonate interference on labile soil organic matter peaks for midDRIFTS analysis, *Soil Biol. Biochem.*, 99, 150–157, doi:10.1016/j.soilbio.2016.05.010, 2016.
- Monteith, J. L.: Evaporation and surface temperature, *Q. J. R. Meteorol. Soc.*, 12, 513–522, doi:10.1002/qj.49710745102, 1976.
- 820 Mualem, Y.: A new model for predicting the hydraulic conductivity of unsaturated porous media, *Water Resour. Res.*, 12(3), 513–522, doi:10.1029/WR012i003p00513, 1976.
- Mueller, T., Jensen, L. S. S., Magid, J. and Nielsen, N. E. E.: Temporal variation of C and N turnover in soil after oilseed rape straw incorporation in the field: simulations with the soil-plant-atmosphere model DAISY, *Ecol. Modell.*, 99(2), 247–262, doi:http://dx.doi.org/10.1016/S0304-3800(97)01959-5, 1997.
- 825 Mueller, T., Magid, J., Jensen, L. S., Svendsen, H. and Nielsen, N. E.: Soil C and N turnover after incorporation of chopped maize, barley straw and blue grass in the field: Evaluation of the DAISY soil–organic-matter submodel, *Ecol. Modell.*, 111(1), 1–15, doi:10.1016/S0304-3800(98)00094-5, 1998.
- Nguyen, T., Janik, L. and Raupach, M.: Diffuse reflectance infrared fourier transform (DRIFT) spectroscopy in soil studies, *Soil Res.*, 29(1), 49, doi:10.1071/SR9910049, 1991.
- 830 Nkwain, F. N., Demyan, M. S., Rasche, F., Dignac, M.-F., Schulz, E., Kätterer, T., Müller, T. and Cadisch, G.: Coupling pyrolysis with mid-infrared spectroscopy (Py-MIRS) to fingerprint soil organic matter bulk chemistry, *J. Anal. Appl. Pyrolysis*, 133(April 2017), 176–184, doi:10.1016/j.jaap.2018.04.004, 2018.
- 835 Nocita, M., Stevens, A., van Wesemael, B., Aitkenhead, M., Bachmann, M., Barthès, B., Ben Dor, E., Brown, D. J., Clairotte, M., Csorba, A., Dardenne, P., Demattê, J. A. M., Genot, V., Guerrero, C., Knadel, M., Montanarella, L., Noon, C., Ramirez-Lopez, L., Robertson, J., Sakai, H., Soriano-Disla, J. M., Shepherd, K. D., Stenberg, B., Towett, E.

- K., Vargas, R. and Wetterlind, J.: Soil Spectroscopy: An Alternative to Wet Chemistry for Soil Monitoring, in *Advances in Agronomy*, vol. 132, pp. 139–159., 2015.
- 840 O’Leary, G. J., Liu, D. L., Ma, Y., Li, F. Y., McCaskill, M., Conyers, M., Dalal, R., Reeves, S., Page, K., Dang, Y. P. and Robertson, F.: Modelling soil organic carbon 1. Performance of APSIM crop and pasture modules against long-term experimental data, *Geoderma*, 264(November 2015), 227–237, doi:10.1016/j.geoderma.2015.11.004, 2016.
- Parton, W. J., Schimel, D. S., Cole, C. V. and Ojima, D. S.: Analysis of Factors Controlling Soil Organic Matter Levels in Great Plains Grasslands<sup>1</sup>, *Soil Sci. Soc. Am. J.*, 51(5), 1173, doi:10.2136/sssaj1987.03615995005100050015x, 1987.
- 845 Parton, W. J., Scurlock, J. M. O., Ojima, D. S., Gilmanov, T. G., Scholes, R. J., Schimel, D. S., Kirchner, T., Menaut, J.-C., Seastedt, T., Garcia Moya, E., Kamnalrut, A. and Kinyamario, J. I.: Observations and modeling of biomass and soil organic matter dynamics for the grassland biome worldwide, *Global Biogeochem. Cycles*, 7(4), 785–809, doi:10.1029/93GB02042, 1993.
- 850 Pengerud, A., Cécillon, L., Johnsen, L. K., Rasse, D. P. and Strand, L. T.: Permafrost Distribution Drives Soil Organic Matter Stability in a Subarctic Palsa Peatland, *Ecosystems*, 16(6), 934–947, doi:10.1007/s10021-013-9652-5, 2013.
- Piepho, H. P., Büchse, A. and Richter, C.: A Mixed Modelling Approach for Randomized Experiments with Repeated Measures, *J. Agron. Crop Sci.*, 190(4), 230–247, doi:10.1111/j.1439-037X.2004.00097.x, 2004.
- 855 Poeplau, C., Don, A., Dondini, M., Leifeld, J., Nemo, R., Schumacher, J., Senapati, N. and Wiesmeier, M.: Reproducibility of a soil organic carbon fractionation method to derive RothC carbon pools, *Eur. J. Soil Sci.*, 64(6), 735–746, doi:10.1111/ejss.12088, 2013.
- Poeter, E. P., Hill, M. C., Banta, E. R., Mehl, S. and Christensen, S.: UCODE\_2005 and six other computer codes for universal sensitivity analysis, inverse modeling, and uncertainty evaluation, *U.S. Geological Survey Techniques and Methods 6-A11*, 283p. (As updated in Feb 2008)., 2005.
- 860 Poeter, E. P., Hill, M. C., Lu, D., Tiedeman, C. R. and Mehl, S.: UCODE\_2014, with New Capabilities to Define Parameters Unique to Predictions, Calculate Weights using Simulated Values, Estimate Parameters with SVD, Evaluate Uncertainty with MCMC, and More, *Integrated Groundwater Modeling Center Report Number: GWMI 2014-02.*, 2014.
- 865 Poyda, A., Wizemann, H.-D., Ingwersen, J., Eshonkulov, R., Högy, P., Demyan, M. S., Kremer, P., Wulfmeyer, V. and Streck, T.: Carbon fluxes and budgets of intensive crop rotations in two regional climates of southwest Germany, *Agric. Ecosyst. Environ.*, 276, 31–46, doi:10.1016/j.agee.2019.02.011, 2019.
- S. Hansen, P. Abrahamsen, C. T. Petersen and M. Styczen: Daisy: Model Use, Calibration, and Validation, *Trans. ASABE*, 55(4), 1317–1335, doi:10.13031/2013.42244, 2012.
- 870 Segoli, M., De Gryze, S., Dou, F., Lee, J., Post, W. M., Denef, K. and Six, J.: AggModel: A soil organic matter model with measurable pools for use in incubation studies, *Ecol. Modell.*, 263, 1–9, doi:10.1016/j.ecolmodel.2013.04.010, 2013.
- Sohi, S. P., Mahieu, N., Arah, J. R. M., Powlson, D. S., Madari, B. and Gaunt, J. L.: A Procedure for Isolating Soil Organic Matter Fractions Suitable for Modeling, *Soil Sci. Soc. Am. J.*, 65(4), 1121, doi:10.2136/sssaj2001.6541121x, 2001.
- 875 Stevenson, F. J.: *Humus chemistry: genesis, composition, reactions*, John Wiley & Sons, New York., 1994.
- Sulman, B. N., Phillips, R. P., Oishi, A. C., Shevliakova, E. and Pacala, S. W.: Microbe-driven turnover offsets mineral-mediated storage of soil carbon under elevated CO<sub>2</sub>, *Nat. Clim. Chang.*, 4(12), 1099–1102, doi:10.1038/nclimate2436, 2014.
- 880 Sulman, B. N., Moore, J. A. M., Abramoff, R., Averill, C., Kivlin, S., Georgiou, K., Sridhar, B., Hartman, M. D., Wang, G., Wieder, W. R., Bradford, M. A., Luo, Y., Mayes, M. A., Morrison, E., Riley, W. J., Salazar, A., Schimel, J. P., Tang,

- J. and Classen, A. T.: Multiple models and experiments underscore large uncertainty in soil carbon dynamics, *Biogeochemistry*, 141(2), 109–123, doi:10.1007/s10533-018-0509-z, 2018.
- 885 Tinti, A., Tugnoli, V., Bonora, S. and Francioso, O.: Recent applications of vibrational mid-infrared (IR) spectroscopy for studying soil components: A review, *J. Cent. Eur. Agric.*, 16(1), 1–22, doi:10.5513/JCEA01/16.1.1535, 2015.
- Vrugt, J. A.: Markov chain Monte Carlo simulation using the DREAM software package: Theory, concepts, and MATLAB implementation, *Environ. Model. Softw.*, 75, 273–316, doi:10.1016/j.envsoft.2015.08.013, 2016.
- 890 Wattenbach, M., Gottschalk, P., Hattermann, F., Rachimow, C., Flechsig, M. and Smith, P.: A framework for assessing uncertainty in ecosystem models, in (eds). *Proceedings of the iEMSs Third Biennial Meeting: “Summit on Environmental Modelling and Software”*. International Environmental Modelling and Software Society, Burlington, USA, July 2006. CD ROM. Internet: <http://www.iemss.org/iemss2006/sessions/all>, 2006.
- Wizemann, H.-D., Ingwersen, J., Högy, P., Warrach-Sagi, K., Streck, T. and Wulfmeyer, V.: Three year observations of water vapor and energy fluxes over agricultural crops in two regional climates of Southwest Germany, *Meteorol. Zeitschrift*, 24(1), 39–59, doi:10.1127/metz/2014/0618, 2015.
- 895 Yeasmin, S., Singh, B., Johnston, C. T. and Sparks, D. L.: Evaluation of pre-treatment procedures for improved interpretation of mid infrared spectra of soil organic matter, *Geoderma*, 304, 83–92, doi:10.1016/j.geoderma.2016.04.008, 2017.
- 900 Zimmermann, M., Leifeld, J., Schmidt, M. W. I., Smith, P. and Fuhrer, J.: Measured soil organic matter fractions can be related to pools in the RothC model, *Eur. J. Soil Sci.*, 58(3), 658–667, doi:10.1111/j.1365-2389.2006.00855.x, 2007.

## 9 Tables

**Table 1** Locations, descriptions, soil type according to (IUSS Working Group WRB, 2007), and initial soil organic carbon (SOC) stocks and other properties of the used simulated bare fallow study sites

Study Site	UTM Degrees Latitude	UTM Degrees Longitude	Soil type	Depth of measurements sampling (cm)	Rep.	Clay (%)	Silt (%)	Initial SOC (%)	Bulk density (Mg/m <sup>3</sup> )	Initial SOC stocks in the measured sampled depth at fallow start (Mg/ha)	Year of experiment and bare fallow establishment	Years of bulk soil samples available from yearsity	Types of available measurements
Ultuna <sup>1</sup> Ultuna	59.821879	17.656348	Eutric Cambisol	0 - 20	<u>4</u>	37	41	1.50	1.44	43.22	<u>1956</u>	1956, 79, 95, 2005	SOC, DRIFTS
Bad Lauchstädt <sup>2</sup>	51.391605	11.877028	Haplic Chernozem	0 - 20	<u>2</u>	21	68	1.82	1.24	45.08	<u>1985</u>	1985, 2001, 04, 08	SOC, DRIFTS
Kraichgau 1	48.928517	8.702794	Stagnic Luvisol	0 - 30	<u>3</u>	18	97	0.90	1.37	37.10	<u>2009</u>	2009 - 16	SOC, DRIFTS, SMB-C
Kraichgau 2	48.927748	8.708884	Stagnic Luvisol	0 - 30	<u>3</u>	18	80	1.04	1.33	41.61	<u>2009</u>	2009 - 16	SOC, DRIFTS, SMB-C
Kraichgau 3	48.927197	8.715891	Stagnic Luvisol	0 - 30	<u>3</u>	17	81	0.89	1.44	38.50	<u>2009</u>	2009 - 16	SOC, DRIFTS, SMB-C
Swabian Jura 1	48.527510	9.769429	Calcic Luvisol	0 - 30	<u>3</u>	38	56	1.78	1.32	70.33	<u>2009</u>	2009 - 16	SOC, DRIFTS, SMB-C
Swabian Jura 2	48.529857	9.773253	Anthrosol	0 - 30	<u>3</u>	29	68	1.95	1.38	80.85	<u>2009</u>	2009 - 13	SOC, DRIFTS, SMB-C
Swabian Jura 3	48.547035	9.773176	Rendzic Leptosol	0 - 30	<u>3</u>	45	51	1.91	1.07	61.27	<u>2009</u>	2009 - 13	SOC, DRIFTS, SMB-C

UTM = Universal Transverse Mercator reference system, SOC= soil organic carbon, Rep.= replicates, SOC = soil organic carbon, DRIFTS = Diffuse reflectance mid infrared Fourier transform spectroscopy, SMB-C = soil microbial biomass carbon, <sup>1</sup> = Ultuna continuous soil organic matter field experiment (Kätterer et al., 2011), <sup>2</sup> = Bad Lauchstädt extreme farmyard manure experiment (Blair et al., 2006)

**Table 2 Values of the two initial DAISY parameter sets for the DAISY SOM model that were used in this study. The parameters consist of turnover rates (k), maintenance respiration (only for SMB, added to the turnover rate), carbon use efficiency (CUE -which divides between carbon assimilated by SMB and lost as CO<sub>2</sub>), the humification efficiency (fSOM<sub>slow</sub>) and microbial recycling (part of SMB going directly back to SMB fast at turnover of either SMB pool). A graphical display of the model structure related to these and pools considered with the most important parameters for within this study is found in Figure 1.**

Parameter	Default DAISY	Bruun (2003)	Unit
kSOM <sub>slow</sub>	2.70 * 10 <sup>-6</sup> #	4.30 * 10 <sup>-5</sup> x	d <sup>-1</sup>
kSOM <sub>fast</sub>	1.40 * 10 <sup>-4</sup> #	1.40 * 10 <sup>-4</sup> #	d <sup>-1</sup>
kSMB <sub>slow</sub>	1.85 * 10 <sup>-4</sup> *	1.85 * 10 <sup>-4</sup> *	d <sup>-1</sup>
kSMB <sub>fast</sub>	1.00 * 10 <sup>-2</sup> *	1.00 * 10 <sup>-2</sup> *	d <sup>-1</sup>
kAOM <sub>slow</sub>	0.012 *	0.012 *	d <sup>-1</sup>
kAOM <sub>fast</sub>	0.05 *	0.05 *	d <sup>-1</sup>
maint_SMB <sub>slow</sub>	1.80 * 10 <sup>-3</sup> *	1.80 * 10 <sup>-3</sup> *	d <sup>-1</sup>
maint_SMB <sub>fast</sub>	1.00 * 10 <sup>-2</sup> *	1.00 * 10 <sup>-2</sup> *	d <sup>-1</sup>
CUE_SMB	0.60 #	0.60 #	kg kg <sup>-1</sup>
CUE_SOM <sub>slow</sub>	0.40 *	0.40 *	kg kg <sup>-1</sup>
CUE_SOM <sub>fast</sub>	0.50 *	0.50 *	kg kg <sup>-1</sup>
CUE_AOM <sub>slow</sub>	0.13 *	0.13 *	kg kg <sup>-1</sup>
CUE_AOM <sub>fast</sub>	0.69 *	0.69 *	kg kg <sup>-1</sup>
fSOM <sub>slow</sub> (humification efficiency)	0.10 #	0.30 x	kg kg <sup>-1</sup>
part_SMB > SOM <sub>fast</sub> (microbial recycling)	0.40 #	0.40 #	kg kg <sup>-1</sup>
fraction of SOM <sub>slow</sub> at steady state Bruun (2002) equation	0.83	0.49	kg kg <sup>-1</sup>

k = turnover rate (=death rate for SMB), maint = maintenance respiration (SMB only), CUE = carbon use efficiency, SOM = soil organic matter pools, SMB = soil microbial biomass pools, AOM = added organic matter pools (not considered in this study), part<sub>i</sub> = partitioning; Source: # original Jensen (1997), \* modified by Müller (1997), x modified by Bruun (2003)

**Table 3** Measured soil properties of the bare fallow experiments at each site at the corresponding to the start of the bare fallow experiment and the end of the end-simulated period. Measurements include SOC and SMB-C stocks in the modeled layer, and the percentage of SOC that would be assigned to the slow pool according to DRIFTS stability index (DSI) measured at 105°C of the bare fallow experiment at each site

Site	Start year of experiment (year)	End year of simulation (year)	Depth of modeled layer (cm)	Bulk density of modeled layer (Mg/m <sup>3</sup> )	SOC at start Mg/ha*	SOC at end Mg/ha*	SMB-C at start Mg/ha*	SMB-C at end Mg/ha*	% DRIFTS SOMC in slow pool at start (DSI 105°C)	% SOC in slow pool at end (DSI 105°C)	% of initial SOC lost	Number of years	% of initial SOC lost per year of initial
Ultuna	1956	2005	0 - 20	1.44	43.22	26.51	NA	NA	54	91	39%	50	0.8%
Bad Lauchstädt	1983	2008	0 - 20	1.24	45.08	41.91	NA	NA	70	80	7%	26	0.3%
Kraichgau 1	2009	2015	0 - 30	1.37	37.10	32.59	0.847	0.408	80	98	12%	7	1.7%
Kraichgau 2	2009	2015	0 - 30	1.33	41.61	38.66	0.853	0.314	73	93	7%	7	1.0%
Kraichgau 3	2009	2015	0 - 30	1.44	38.50	35.06	0.672	0.261	76	99	9%	7	1.3%
Swabian Jura 1	2009	2015	0 - 30	1.32	70.33	63.29	1.566	0.654	64	83	10%	7	1.4%
Swabian Jura 2	2009	2013	0 - 30	1.38	80.85	79.61	1.805	0.970	66	83	2%	5	0.3%
Swabian Jura 3	2009	2013	0 - 30	1.07	61.27	70.29	1.350	0.990	61	76	-15%	5	-2.9%

SOC = soil organic carbon, SMB-C = soil microbial biomass carbon, DSI = Diffuse reflectance mid infrared Fourier transform spectroscopy stability index, NA = no data available for this site, \*stocks in Mg/ha refer to stocks within the depth of the modelled layer

**Table 4. Effect of the initialization method on simulation errors. Displayed are estimated least square means of the (back transformed) absolute error of DAISY bare-fallow simulations for SOC and SMB-C for the sites of Ultuna, Bad Lauchstädt and Kraichgau + Swabian Jura combined. The values Means are the estimate for the end of the simulation period (number of years in brackets). Different capital letters indicate significant differences ( $p < 0.05$ ) within columns (not tested between sites). For Bad Lauchstädt, the initialization effect was non-significant, so only the least square means for the effect of the parameter set is displayed.**

Parameter set	Initialization method of SOM pools	Ultuna (50yr)	Bad Lauchstädt (23yr)	Kraichgau + Swabian Jura (7 yr)	Kraichgau + Swabian Jura (7 yr)
		Least square means of errors (SOC Mg/ha)	Back transformed least square means of errors (SOC Mg/ha)	Back transformed least square means of errors (SOC Mg/ha)	Least square means of errors (SMB-C Mg/ha)
Mueller (1997)	ratio of steady state assumption	13.91 <sup>A</sup>		4.50 <sup>A</sup>	0.354 <sup>A</sup>
	band peak area ratio of DRIFTS at 32°C	10.86 <sup>B</sup>	2.22 <sup>A</sup>	4.50 <sup>A</sup>	0.317 <sup>AB</sup>
	band peak area ratio of DRIFTS at 65°C	10.06 <sup>C</sup>		4.42 <sup>A</sup>	0.274 <sup>ABC</sup>
	band peak area ratio of DRIFTS at 105°C	8.52 <sup>D</sup>		4.28 <sup>A</sup>	0.205 <sup>CD</sup>
Bruun (2003)	ratio of steady state assumption	5.84 <sup>H</sup>		3.12 <sup>B</sup>	0.231 <sup>BCD</sup>
	band peak area ratio of DRIFTS at 32°C	7.06 <sup>E</sup>	6.01 <sup>B</sup>	3.31 <sup>B</sup>	0.179 <sup>CDE</sup>
	band peak area ratio of DRIFTS at 65°C	6.75 <sup>F</sup>		3.30 <sup>B</sup>	0.160 <sup>DE</sup>
	band peak area ratio of DRIFTS at 105°C	6.15 <sup>G</sup>		3.25 <sup>B</sup>	0.131 <sup>E</sup>

SOM = soil organic matter pools.



SOC = soil organic carbon, SMB-C = soil microbial biomass carbon, DRIFTS = Diffuse reflectance mid infrared Fourier transform spectroscopy

**Table 5** ~~Optimized turnover rates and humification efficiency of this study (of this study using the combined site analysis with original weighting and DSI) compared to other Bayesian calibrations and standard values of commonly used models. If the temperature function was given or site temperature specified, the turnover rates of other models were normalized with an exponential equation to the DAISY standard of 10°C using an exponential equation (exception (Clifford et al., 2014), where no temperature was given) which is standard in DAISY.~~

Model	DAISY	ICBM	CBM-CFS3	APSIM	own creation*	CENTURY	DAISY	DAISY
Reference	This study	Ahrens	Hararuk	Luo	Clifford	Parton	Mueller	Bruun
Year	2019	2014	2017	2016	2014	1993	1997	2003
Turnover rates of the fast pool <del>at 10°C (recalculated to d<sup>-1</sup> at 10°C)</del>								
minimum	1.07 * 10 <sup>-4</sup>	4.57 * 10 <sup>-4</sup>	6.30 * 10 <sup>-4</sup>	NA	NA—no			
optimum	2.29 * 10 <sup>-4</sup>	4.57 * 10 <sup>-3</sup>	1.97 * 10 <sup>-4</sup>	NA	temperature	9.32 * 10 <sup>-5</sup>	1.40 * 10 <sup>-4</sup>	1.40 * 10 <sup>-4</sup>
maximum	3.27 * 10 <sup>-4</sup>	2.28 * 10 <sup>-2</sup>	1.05 * 10 <sup>-3</sup>	NA	found			
Turnover rates of the slow pool <del>at 10°C (recalculated to d<sup>-1</sup> at 10°C)</del>								
minimum	2.99 * 10 <sup>-6</sup>	4.57 * 10 <sup>-7</sup>	9.86 * 10 <sup>-6</sup>	1.00 * 10 <sup>-4</sup>	1.10 * 10 <sup>-4</sup>			
optimum	3.25 * 10 <sup>-5</sup>	2.28 * 10 <sup>-5</sup>	1.10 * 10 <sup>-5</sup>	3.00 * 10 <sup>-4</sup>	1.67 * 10 <sup>-4</sup>	2.10 * 10 <sup>-6</sup>	2.70 * 10 <sup>-6</sup>	4.30 * 10 <sup>-5</sup>
maximum	6.14 * 10 <sup>-5</sup>	4.57 * 10 <sup>-5</sup>	1.32 * 10 <sup>-5</sup>	6.00 * 10 <sup>-4</sup>	2.19 * 10 <sup>-4</sup>			
Portion of fast to slow pool = (humification efficiency (dimensionless))								
minimum	0.05	0.05						
optimum	0.34	0.2				0.3	0.1	0.3
maximum	0.35	0.35						

References: (Ahrens et al., 2014; Bruun et al., 2003; Clifford et al., 2014; Hararuk et al., 2017; Luo et al., 2016; Mueller et al., 1997; Parton et al., 1993). \* remarks – Clifford et al. (2014) did not specify a base temperature for their model

## 10 Figures

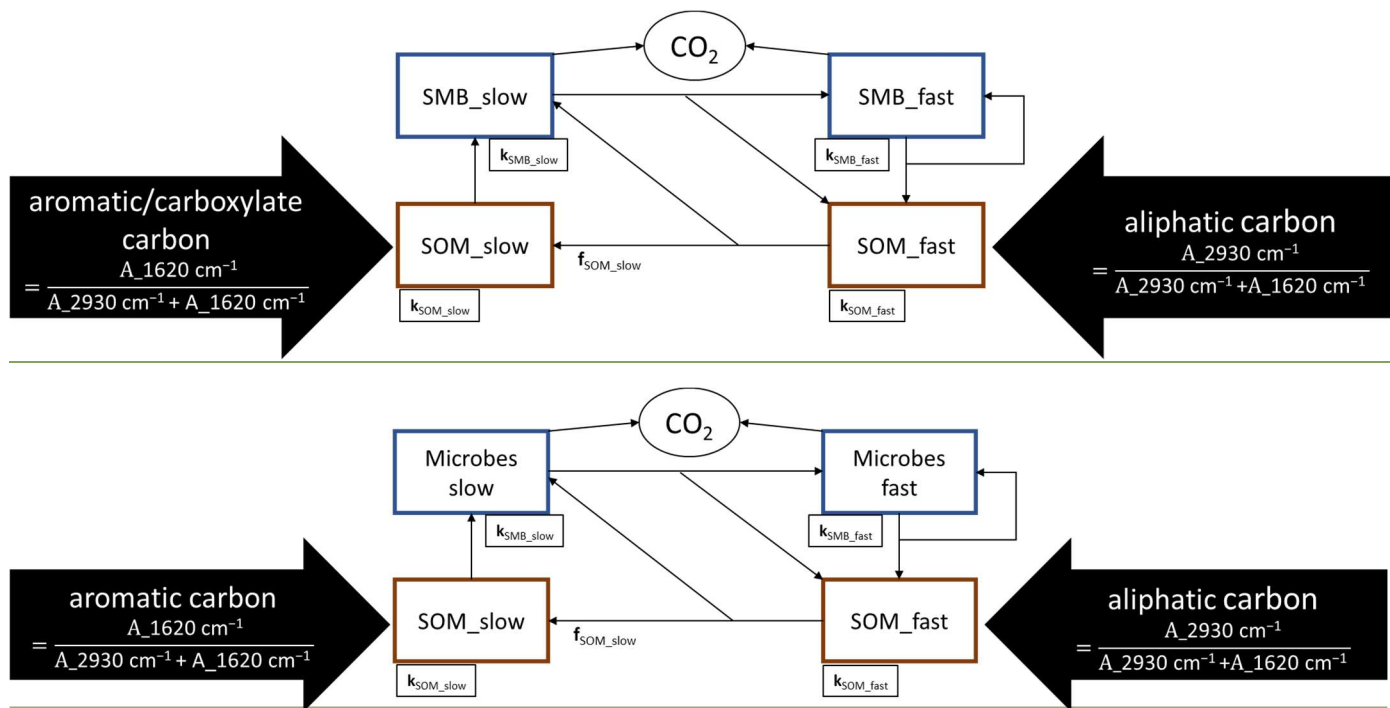


Figure 1 Original structure of the internal cycling of SOM in the DAISY model, as it was used in this study.  $A_{2930} \text{ cm}^{-1}$  and  $A_{1620} \text{ cm}^{-1}$  refer to the areas of below each the DRIFTS absorption bands at  $2930 \text{ cm}^{-1}$  and  $1620 \text{ cm}^{-1}$  (Equation 3), peak obtained by DRIFTS.  $k_{SOM}$  and  $k_{SMB}$  (fast/slow) are turnover rates of the fast and slow SOM and SMB pools, respectively and  $f_{SOM\_slow}$  is the humification efficiency. Other All model parameters can be found in Table 2.

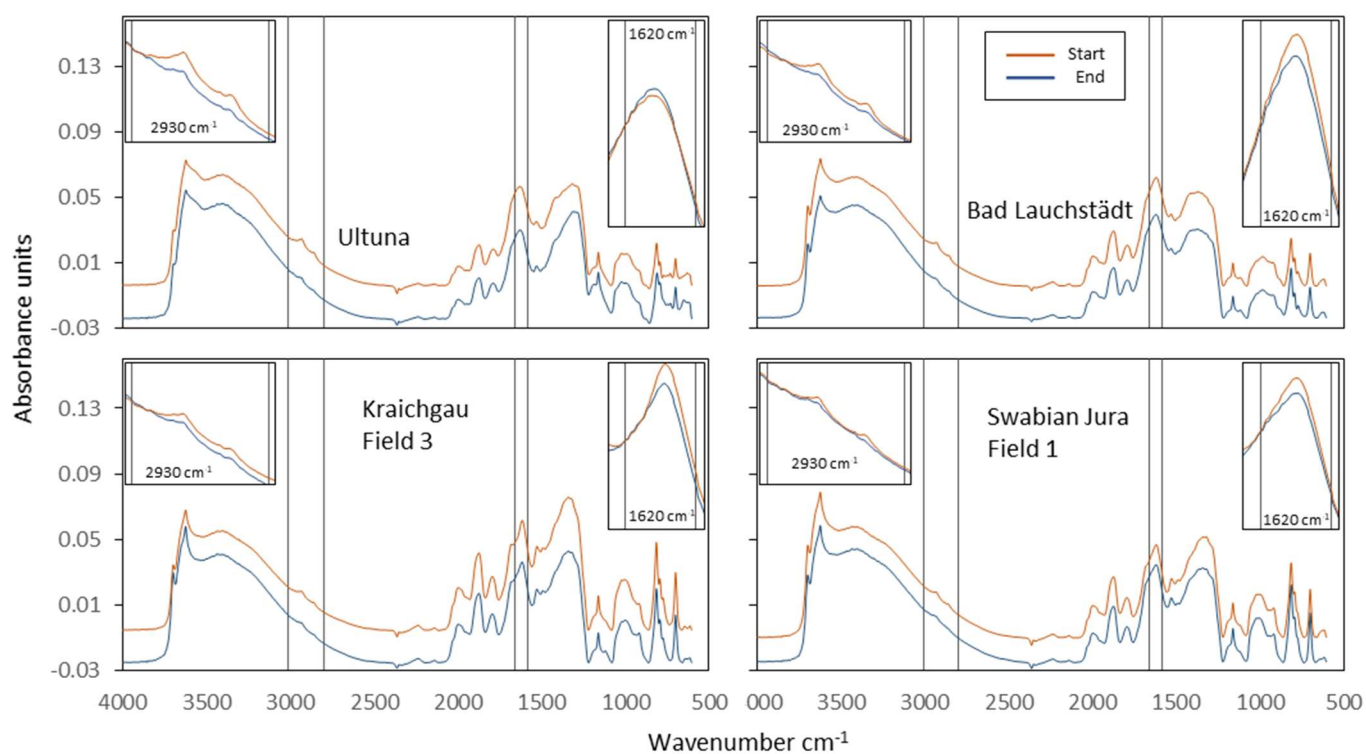
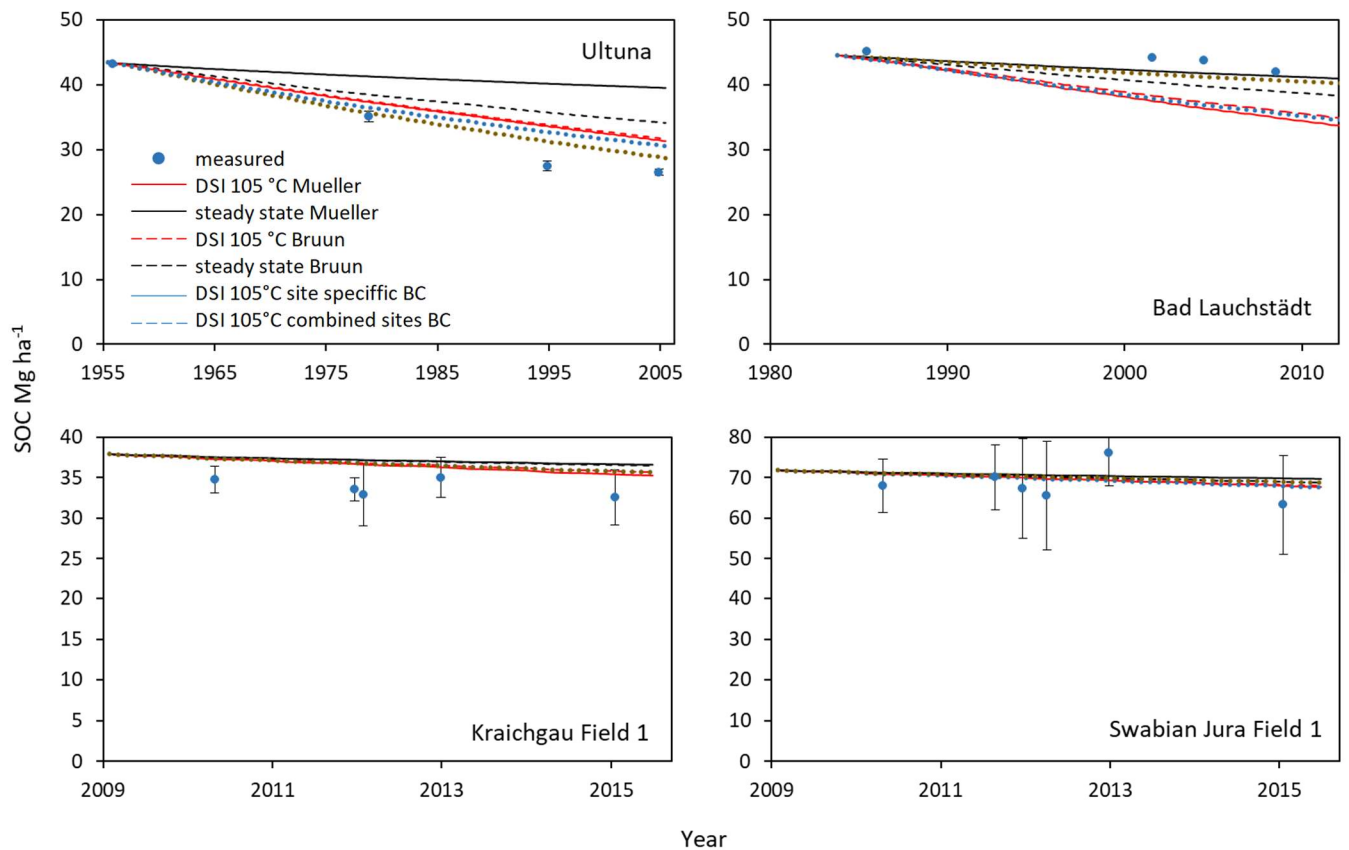
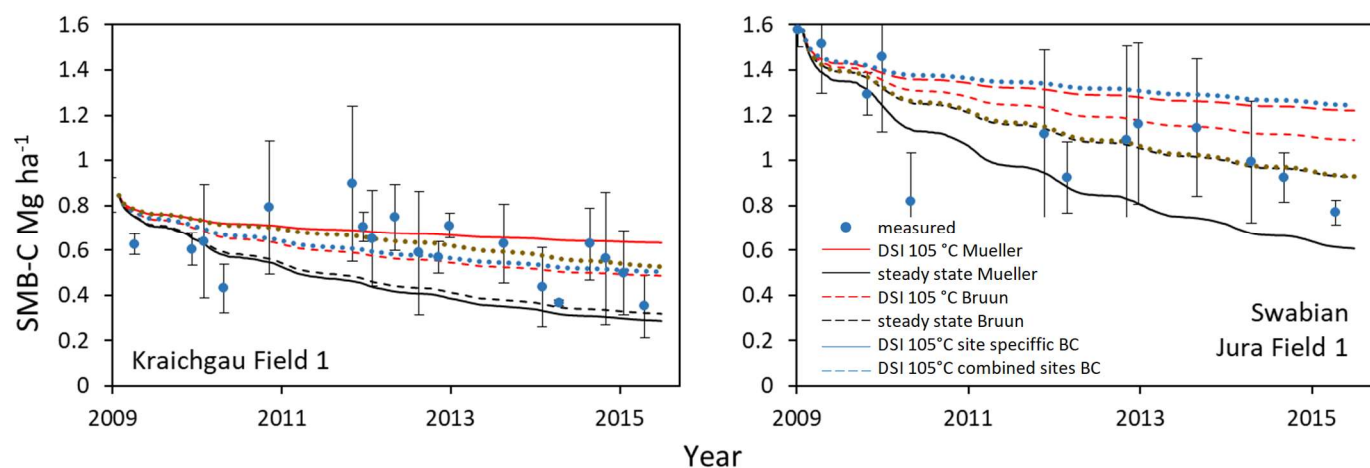


Figure 2 **Examples of DRIFTS baseline corrected and vector normalized examples of DRIFTS spectra of bulk soil samples (dried at 105°C) of the first and last year of the bare fallow plots at four sites. Fallow periods were 50 years (Ultuna), 24 years (Bad Lauchstädt) and 7 years (Kraichgau and Swabian Jura). Small pictures on the top left and right, are zoomed in versions of the 2930cm<sup>-1</sup> band peak and the 1620cm<sup>-1</sup> band peak, respectively. For better visibility, the full spectra pictures have a y-axis offset (+0.02 for samples from the start), while zoomed in versions share a common baseline. More details on the sites in Table 3.**



**Figure 3** Example of SOC simulations from Ultuna (top left), Bad Lauchstädt (top right), Kraichgau field 1 (bottom left) and Swabian Jura Field 1 (bottom right). Initializations were done (i) assuming steady state using the formula of Bruun and Jensen (2002) (equation 1) with both turnover rates of Mueller et al. (1997) and Bruun et al. (2003) and (ii) by the DRIFTS stability index (DSI) at 105°C drying temperature using both turnover rates for simulations (simulations using the other drying temperatures for DSI in the supplementary). The site specific and the combination of all sites Bayesian calibrations (BC) are also displayed. Bars indicate the standard deviation of measured values of all plots (n = 3) per field.



**Figure 4** Example SMB-C simulations for Kraichgau field 1 (left) and Swabian Jura Field 1 (right). Initializations were done (i) assuming steady state using the formula of Bruun and Jensen (2002) with turnover rates of Mueller et al. (1997) and Bruun et al. (2003) and (ii) by the DRIFTS stability index (DSI) at 105°C drying temperature using both turnover rates for simulations (simulations using the other drying temperatures for DRIFTS in the supplementary). The site specific and the combination of all sites Bayesian calibrations (BC) are also displayed. Bars indicate the standard deviation of measured values of all plots (n = 3) per field.

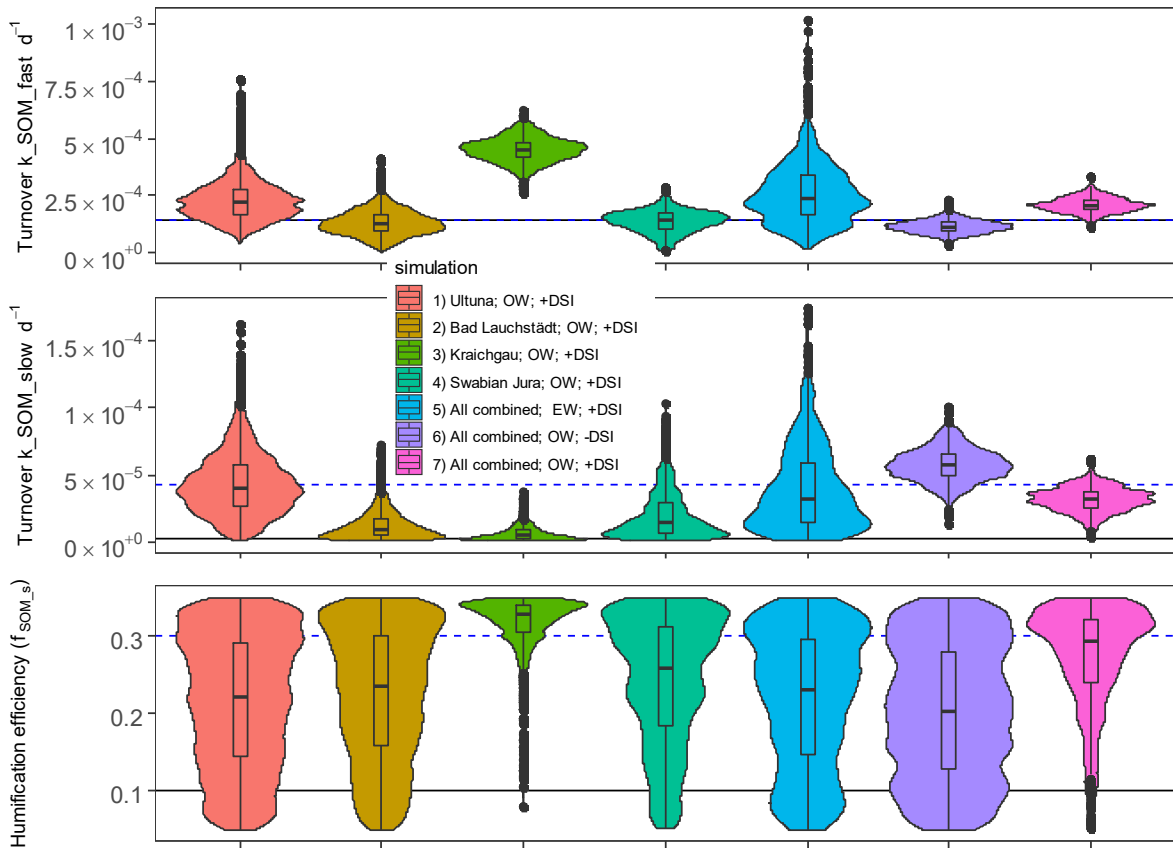


**Figure 5** Violin plots of the parameter distributions, obtained by the Bayesian calibration using only the individual sites (1-4) and all sites combined (5-7) with different weighing schemes (OW = original weight, EW = equal weight calibration; +/- DSI indicates, whether the DSI data was used for calibration). The black line corresponds to the parameters of Mueller (1997), the blue dashed line to the parameters of Bruun (2003). Note: The turnover  $k_{SOM\_fast}$  parameter (top figure) is the same in both Mueller (1997) and Bruun (2003)

a)

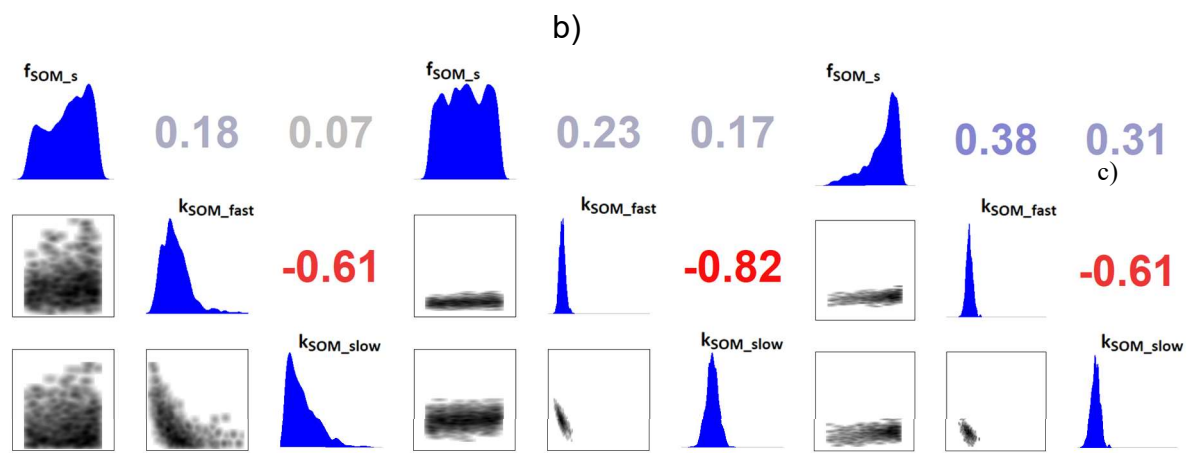


Figure 6 Correlation matrices of posterior distributions from the Bayesian calibrations of a) equal weight calibration for all sites combined using DSI (5), b) original weight calibration for all sites combined without using DSI (6), and c) original weight calibration for all sites combined using the DSI (7). The plots of individual site simulations (1-4) can be found in the supplemental material.

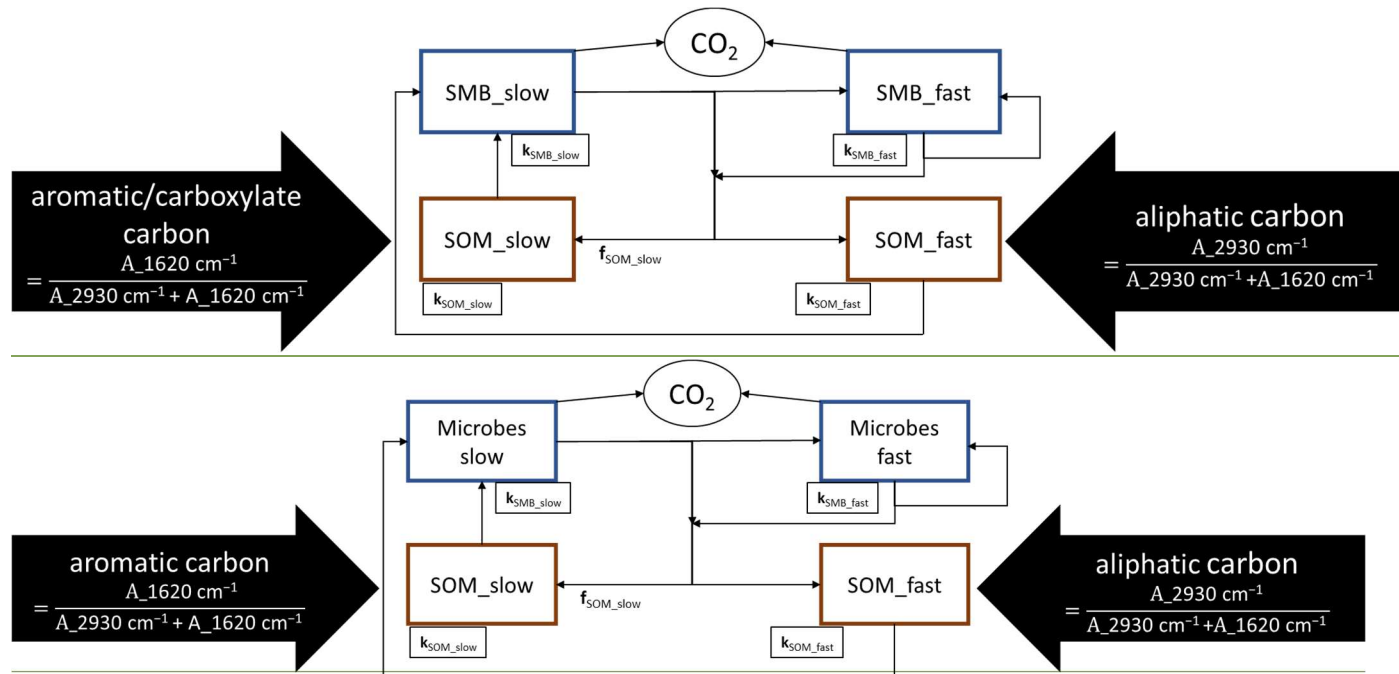


Figure 7 Suggested improvements to the internal cycling structure of SOM in the DAISY model. The division into fast and slow cycling SOM, corresponding to aliphatic-aliphatic and aromatic-aromatic/carboxylate carbon happens follows the turnover at the death of either microbSMB pools. Aliphatic-Aliphatic carbon no longer becomes complex aromatic/carboxylate carbon without the involvement of microbes.